Extraction and nanoparticle preparation of natural materials by using supercritical carbon dioxide

Chiho UEMORI

Extraction and nanoparticle preparation of natural materials by using supercritical carbon dioxide

March 2018

Chiho UEMORI

Department of Chemical Engineering
Graduate School of Engineering
Nagoya University

Content

Chapter 4

Crystallization of acetaminophen using swirl mixing micro device

Chapter 5

Production of Liposome from Sphingomyelin by Ultrasonic Device under Supercritical Carbon Dioxide

Chapter 6

Summary and Conclusions

Chapter 1

Introduction

1-1. Introduction

Recently, practical application of supercritical fluid has been developed rapidly. However, since the supercritical fluid has high pressure and high temperature, it is often regarded as special physical properties. Over 30 years have passed since the research on supercritical fluids has started in Japan, and various related technologies have been developed in the field of separation, reaction, and material processing. For example, extraction of valuable components using supercritical carbon dioxide or chemical reaction using supercritical water or alcohol. Supercritical fluid technologies are focused especially from the view point of environmental burden. Further attention is being paid as a material processing medium for nanostructures. More research and development in Asia have been progressed in recent years from fundamental study to commercialization. Subcritical liquids and gases below the critical point can also be used as a reaction media.

However, from the viewpoint of engineering knowledge, supercritical fluid technology is not currently constructed as a versatile technology. In this research, we show the process basic design of supercritical fluid for separation and particle formation.

1-2. Supercritical Fluid

A supercritical fluid is defined as a noncondensable fluid. Supercritical fluid is beyond the critical points of gas and liquid in terms of temperature and pressure. The supercritical region is present in all substances. Because it exceeds the critical point, molecular motion is intense. Furthermore, it is possible to change the density from a state close to a gas to a state close to a liquid. This is related to the change of the equilibrium physical property such as solvency and ion product and transport property such as diffusion coefficient. The transport properties can be controlled by changing temperature and pressure. The phase state of the substance is determined by the force between the molecules constituting the substance and the force that the molecule tries to diffuse due to the thermal motion. It is the balance between intermolecular force and molecular diffusion. The intermolecular force is considered to be determined by the molecular distance. As a result, molecular dynamics are much greater for dense solids or liquids than for gases. In the gas phase, it becomes larger as the pressure becomes higher.

Carbon dioxide is commonly used as a supercritical fluid. Water and alcohols such as methanol are also used. Supercritical carbon dioxide has a low polarity and is used as extraction solvent for low polar compounds. For polar compounds, polar entrainer such as ethanol and water is added to carbon dioxide. It is also used for material processing such as micronization

and aerogel production. Supercritical water is highly reactive and is used for decomposition of organic substances and detoxification of harmful substances.

Measurement of physical properties of supercritical fluid has being carried out extensively. At constant pressure, density decreases with increasing temperature. In the vicinity of the critical point, the density varies greatly by minute changes in temperature and pressure.

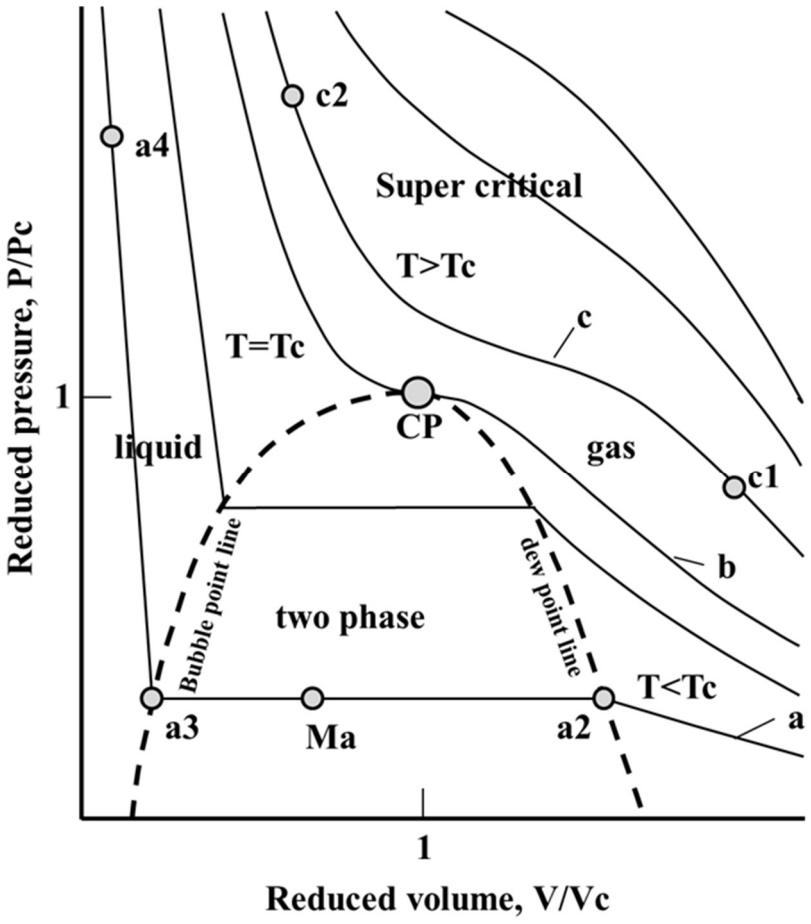

Fig. 1-1. Relationship between pressure, specific volume and temperature of fluid

The behavior of the isotherm is shown in **Fig. 1-1**. In the critical temperature, the inflection point is taken. Below the critical temperature the gas volume decreases with increasing pressure and reaches saturated vapor. In the **Figure**, **a3** indicates the boiling point, and between **a2** and **a3** is the gas-liquid coexisting state.

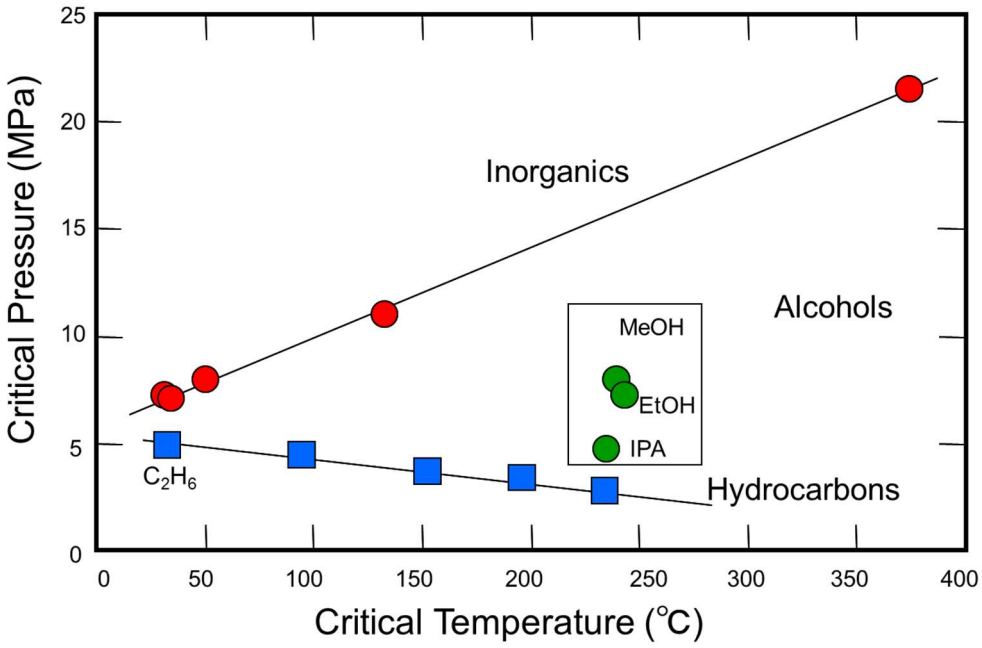

Fig. 1-2 Relationship between critical temperature and critical pressure of substance

Fig. 1-2 shows the relationship between critical temperature and critical pressure of substance. For inorganic substances such as carbon dioxide and water, the critical pressure increases linearly with the critical temperature.

On the other hand, hydrocarbon substances such as methane are reversed. Alcohols are in a substantially constant critical temperature range, and the critical pressure correlates with its molecular weight.

1-3. Supercritical CO_2 extraction

Supercritical carbon dioxide has a critical temperature of 31 °C and materials can be processed at low temperature. It is suitable for the treatment of substances subject to thermal denaturation such as foods and pharmaceuticals. Carbon dioxide is a normally inactive substance. It is further characterized by being tasteless and odorless. It is close to nonpolarity and has characteristics similar to organic solvents such as hexane. Since it is a gas at ambient temperature and pressure, separation of carbon dioxide from the processed products is simple.

It is possible to control the dissolving power by changing the temperature and pressure. Supercritical carbon dioxide has a very high solubility for liposoluble substances with small polarity. On the other hand, polar substances, inorganic salts, proteins and sugars are hardly soluble. When processing these low solubility substances, water or ethanol is used as entrainer. When it is used for extraction process, after extraction at high pressure, by reducing to low pressure carbon dioxide solvent is eliminated as

gas. Therefore, the safety of the solvent is very high. Since supercritical carbon dioxide may permeate into polymers, it is also possible to expand and process the polymer.

1-4. Micronization using supercritical carbon dioxide

Techniques using supercritical carbon dioxide include fine particle production. This is based on phase separation by pressure manipulation. Among various methods using supercritical fluid, there are a method of atomization such as rapid expansion of supercritical solution (RESS) and a method of anti-solvent such as supercritical anti-solvent recrystallization (SAS). Changes in temperature and pressure are factors for promoting solubility of supercritical fluid, resulting to nucleation and crystal growth. Changes in solubility are related to fine particle production. We have studied several methods of fine particle production such as carotenoids, pharmaceuticals, and liposome.

Chapter 2

Phytochemicals extraction from Grains of Paradise

2-1. Grains of Paradise

The genus Zingiberaceae contains between 40 and 50 species perennial herbs, native to Africa. As one of Zingiberaceae species, grains of paradise (*Aframomum melegueta* [Rosco] K. Schum.) generally referred to as guinea grains or alligator pepper or melegueta pepper is a perennial herb with short rhizomes from which arise distinct leafy shoots, 1.5 – 2 m. Grains of paradise is native to West Africa, and cultivated in Ghana, Guinea, the Ivory Coast, Nigeria and Sierra Leone [1]. The seeds of grains of paradise, source of melegueta pepper, are used as a spice for flavoring food and have wide range of ethnobotanical uses.

Phenolic compounds are known as the most abundant secondary metabolites of plants. These compounds were a phytochemicals group which have a phenol structure and considered as important determinants in the nutritional and the quality of fruits, vegetables, other plant foods, and food preparations. Phenolic compounds were widely found in the plant world and commonly involved in defense toward ultraviolet radiation or attack by pathogens, parasites, and predators [2]. Hence, these compounds play an important role in plant growth and offer the plants to have excellent properties as food preservatives. Phenolic compounds were also affect to the color and contribute to sensory characteristics of vegetables and fruits [3]. Due to these properties, phenolic compounds become suitable for various

industrial applications such as natural colorants and preservatives for foods or in the production of paints, paper, and cosmetics. As one of the spice plants, grains of paradise was also contained of phenolic compounds such as gingerols, shogaols, and paradols [4,5]. These phenolic compounds have various biological properties especially in anti–inflammatory, anti–oxidant and anti–tumor effects. As one of potent nutraceuticals, 6–gingerol had a variety of pharmacological abilities and has been known to have anti–hyperglycemic, anti–cancer and anti–oxidative properties [6]. 6–shogaol also was known as anti–proliferative, anti–metastatic, and pro-apoptotic activities via suppression of STAT3 gene products in tumor tissues [7]. It effectively decreased survival and affected apoptosis process in human and mouse prostate cancer cells via inhibition of STAT3 and NF–κB activities. Compared with 6–paradol which found in grains of paradise seeds, 6–shogaol was more effective [8]. 6–shogaol may also prevent the growth of human pancreatic tumors and has a high responsive to gemcitabine by suppressing inflammatory pathways linked to tumorigenesis [9].

In the present work, supercritical carbon dioxide ($SCCO_2$) was employed as a solvent extraction [10–14] to extract phenolic compounds from grains of paradise seeds. The $SCCO_2$ extraction technique is very advantageous and environmentally friendly compared with other conventional extraction technique, such as soxhlet extraction technique. Due to its high diffusivity combined with its high solvent strength that can be easily tuned by changing of temperature and/or pressure, $SCCO_2$ became an

attractive extraction medium. At room temperature and ambient pressure, CO_2 has gaseous phase so it can be easily separated and recycled as the solutes dissolved in the $SCCO_2$ will precipitate upon depressurization. Accordingly, supercritical fluid extraction including $SCCO_2$ may offer appropriate technique for extraction and fractionation seem to be promising for the food and pharmaceutical industries and to be more efficient extraction fluids than traditional liquid solvents [14].

2-2. Experimental Section

2-2-1. Materials

Dried seeds of grains of paradise were obtained from south of Nigeria. Prior to extraction, the seeds were ground with a grinder (IKA, MF–10–B–S1, USA) into certain particle size and passed through fine–mesh sieves (MF–Sieb 0.25 mm, Germany). 6–gingerol ($C_{17}H_{26}O_4$; 98%) and 6–shogaol ($C_{17}H_{24}O_3$; 98%) were obtained from Tokiwa Phytochemical Co., Ltd (Tokyo, Japan) and 6–paradol ($C_{17}H_{26}O_3$) with purity of 98.0 % was purchased from Medchemexpress (MCE) LLC, USA. Ethanol (C_2H_6O; 99.5%) was purchased from Nacalai Tesque (Japan) and acetonitrile (C_2H_3N; HPLC grade) obtained from Wako Pure Chemicals Industries Ltd., Japan. All chemicals were used without further purification. Carbon dioxide (CO_2: 99%) was supplied by Sogo Kariya Sanso, Inc. Japan.

2-2-2. Experimental setup and procedure

Fig. 2-1 showed the schematic diagram of $SCCO_2$ extraction apparatus which used in these experiments. The apparatus includes a high–pressure pump for CO_2 (PU–2086; Jasco, Japan), a heating chamber (WFO–400; EYELA, Tokyo, Japan), a 10 mL extraction cell (Thar Technologies, Inc., PA, USA) and back pressure regulator (AKICO, Tokyo, Japan). In this work, the extraction of 6–gingerol, 6–shogaol, and 6–paradol from grains of paradise seeds by $SCCO_2$ was carried at temperatures of 40 – 80 ^{o}C and pressures of 20 – 40 MPa using a semi-continuous flow–type system with CO_2 flow rate of 3 mL min^{-1}. 1.0 g of dried grains of paradise seeds were placed into the extractor, the glass beads were also filled at the bottom and top of the extractor in each experiment. The extractor was put in the heating chamber to keep the operating temperature. The extraction process can be explained briefly as follow. The dried grains of paradise seeds were filled into the extractor and put in the chamber. After the temperature at chamber heater achieved to the desired temperature, CO_2 from a cylinder was firstly liquefied and then pumped into the extractor. In all experiments, the extraction products which trapped in 10 ml ethanol were collected for 180 min, weighed and directly stored in the refrigerator at 5 ^{o}C. The bottles used for the collection of extracts were wrapped in aluminum foil. These processes were done until analysis.

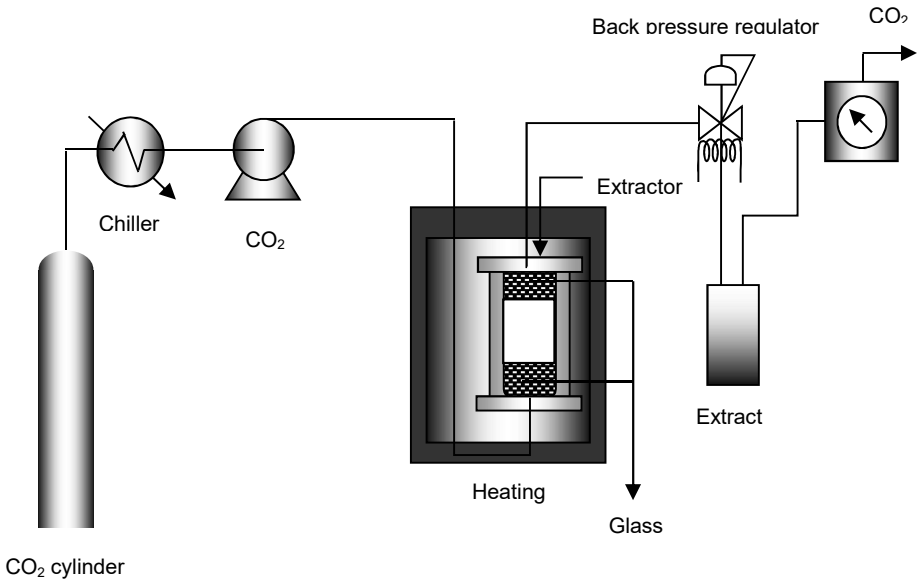

Fig. 2-1. Schematic diagram of $SCCO_2$ extraction system.

2-2-3. Analytical methods

Extracted polyphenolic compounds in the extracts were identified by GC–MS (HP model 6890 series GC system and 5973 mass selective detector) with a HP–5 MS capillary column (J&W Scientific, length 30 m, i.d. 0.32 mm, film thickness 0.25 μm). The temperature program was 1.0 min at 45 °C, 5 °C/min to 270 °C, and 10 min at 270 °C. Helium carrier gas was used at a flow rate of 1.5 mL/min. The NIST (National Institute of Standards and Technology) library of mass spectroscopy was used for identification of the compounds. Quantitavely, extracted polyphenolic compounds in the extracts were analyzed by HPLC LC–10AD equipped with Diode Array Detector SPD–M10A (Shimadzu, Japan). 10 μl of extract dissolved in ethanol was injected by SIL–10AF auto–sampler (Shimadzu, Japan) and separated with a STR

ODS II column (5 μm; 4.6 x 250 mm; Shinwa Chemical Industries, Ltd., Japan) at room temperature. Elution was obtained by using the following gradient steps of solvents A (water) and B (acetonitrile): 0–25 min, 90% B; 25–30 min, 100% B; 30–40 min, 30% B at a flow rate of 1 ml/min. All analyses were carried out under isothermal conditions at 40 °C.. 6–gingerol, 6–shogaol, and 6–paradol were detected at wavelength of 280, 280, and 220 nm, respectively. Solid residues collected at each operating temperature were dried overnight in the oven at 60 °C. Then, they were characterized by using a Spectrum Two FT–IR spectrophotometer (Perkin–Elmer Ltd., England), in order to determine their structure following $SCCO_2$ treatment. Spectra were measured in attenuated total reflectance (ATR) mode (golden single reflection ATR system, P/N 10500 series, Specac) at 4 cm^{-1} resolution. The scanning wave number ranged from 4000 to 400 cm^{-1}. The morphologies of the grains of paradise seeds before and after treatment by $SCCO_2$ were also observed by using a scanning electron microscope (SEM; JEOL JSM–6390LV).

2-3. Results and discussion

In order to understand the change of grains of paradise seeds functional groups during extraction process, the grains of paradise seeds before and after $SCCO_2$ extraction process were subjected into an infrared spectrometer. Here, the grains of paradise seeds that remained after $SCCO_2$ treatment is referred to as solid residue; the solid residue at each extraction condition was then characterized by infrared spectroscopy in the wavenumber region of 4000 –

400 cm^{-1}. **Fig. 2-2** and 3 showed the spectral features of grains of paradise seeds and its solid residue after treatment by $SCCO_2$ at various extraction conditions. Similar to other plant biomass, the chemical compositions of grains of paradise seeds are fairly similar although with different magnitudes of components. The major components of them are cellulose, hemicellulose and lignin. Therefore, the same spectral characteristics of grains of paradise seeds and their solid residues were found. These spectral characteristics also showed that the $SCCO_2$ extraction treatment on the grains of paradise seeds does not change the distribution of their functional groups. However, since the removing or reducing grains of paradise seeds components occurred during extraction process, the different peak intensities of them could be found obviously. It indicated that $SCCO_2$ may extract the chemical compounds from grains of paradise seeds [14–17].

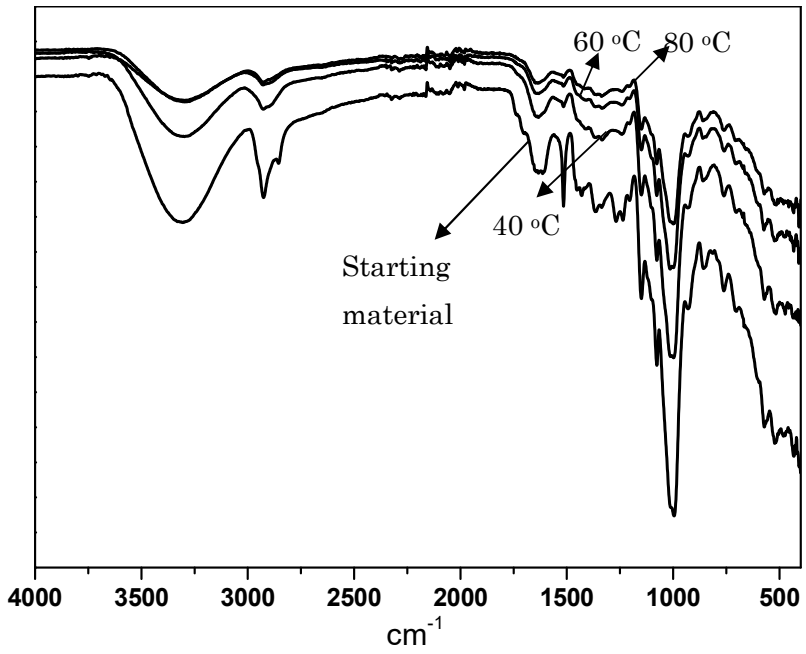

Fig. 2-2. FT–IR spectrum of grains of paradise before and after treatment by $SCCO_2$ at pressure of 30 MPa.

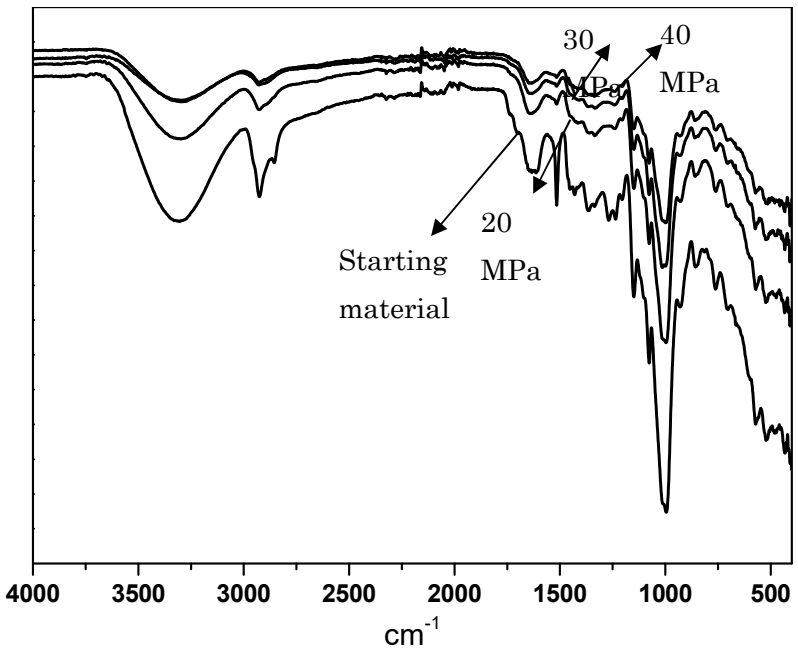

Fig. 2-3. FT–IR spectrum of grains of paradise before and after treatment by $SCCO_2$ at temperature of 40 °C.

Table 2-1. Wave number assignments of FTIR spectra.

Wave number [cm^{-1}]	Functional groups	Compounds
3305	O–H stretching	Acid, methanol
2925	C–H_n stretching	Alkyl, aliphatic, aromatic
1515	C = O stretching	Ketone and carbonyl
1613	C = C stretching	Aromatic skeletal mode
1515	C = O stretching	Ketone and carbonyl
1149	C–O–C stretching vibration	Pyranose ring skeletal
1076	C–O stretching and C–O deformation	C–OH (ethanol)
995	C–N stretching	aliphatic amine

Extraction, in principle, could be expressed as the removal of soluble substances from an insoluble materials, either liquid or solid, by treatment with a liquid solvent. The process might happen when the solvent is flowed in the plants matter at high pressures and/or high temperatures. So, the extraction process will also occur when the carbon dioxide was flowed into the plant materials at high temperatures and/or high pressures due to the change of solvent power that can have a strong influence on extraction process [14,18,19]. **Fig. 2-2** showed the FT–IR spectra of grains of paradise seeds and their solid residues after treatment by $SCCO_2$ when the extraction processes were conducted at various extraction pressures with a constant temperature. This figure clearly revealed that the compositional changes in the each sample (grains of paradise seeds and their solid residues) after applied $SCCO_2$ extraction. The intensities of several functional groups in the grains of paradise seeds decreased at after treatment by $SCCO_2$. **Table 2-1** showed the typical functional groups and the infrared signal with the possible compounds [20,21]. The intensity of the broad band located at 3305 cm^{-1} which was attributed to O–H stretching of hydrogen-bonded hydroxyl groups and the band at 2925 cm^{-1} was representative of C–H stretching became decline and narrow after applied $SCCO_2$ extraction. This indicated that they have been removed during the application of $SCCO_2$ extraction treatment on the grains of paradise seeds. The same phenomenon was also found in other functional groups. As shown in the **Fig. 2-2**, the intensities of them decreased obviously after treatment by $SCCO_2$. It is well known that the extraction temperature and/or pressure are two most important parameters in the $SCCO_2$ due to it

was the major determinants of solvent power that could have a strong effect on effectivity of extraction process. Herrero *et al.* 2010 [22] informed that an increase in extraction temperature at constant extraction pressure leads to a decrease in the density of the $SCCO_2$ and thus its solvatation capacity, nevertheless, an increase in extraction temperature was followed by an increase in vapour pressure of solutes, resulting in a high solubility in the $SCCO_2$. As a result, the grains of paradise seeds components were extracted easily by $SCCO_2$ at a higher extraction temperatures.

Similar to extraction temperature, extraction pressure is also a dominant parameter in the $SCCO_2$ extraction system. An increase in extraction pressure a constant extraction temperature promotes to increasing the density of $SCCO_2$; at the same time, the diffusion coefficient of $SCCO_2$ decreased. A decrease in the $SCCO_2$ diffusion coefficient leads to a lower ability of the CO_2 to penetrate the grains of paradise seeds causing a decrease in the extraction efficiency. However, an increase in the density of the $SCCO_2$ extraction system leads to an increase of its solvating power, thus the enhancement of the extraction efficiency might be occurred. As shown in the **Fig. 2-3**, the intensities of functional groups in the grains of paradise seeds also decreased after treatment by $SCCO_2$ at a constant extraction temperature with the elevating extraction pressures [22]. Judging from these results, it could be said that the changing of extraction temperature and/or pressure could give a strong influence on $SCCO_2$ extraction system.

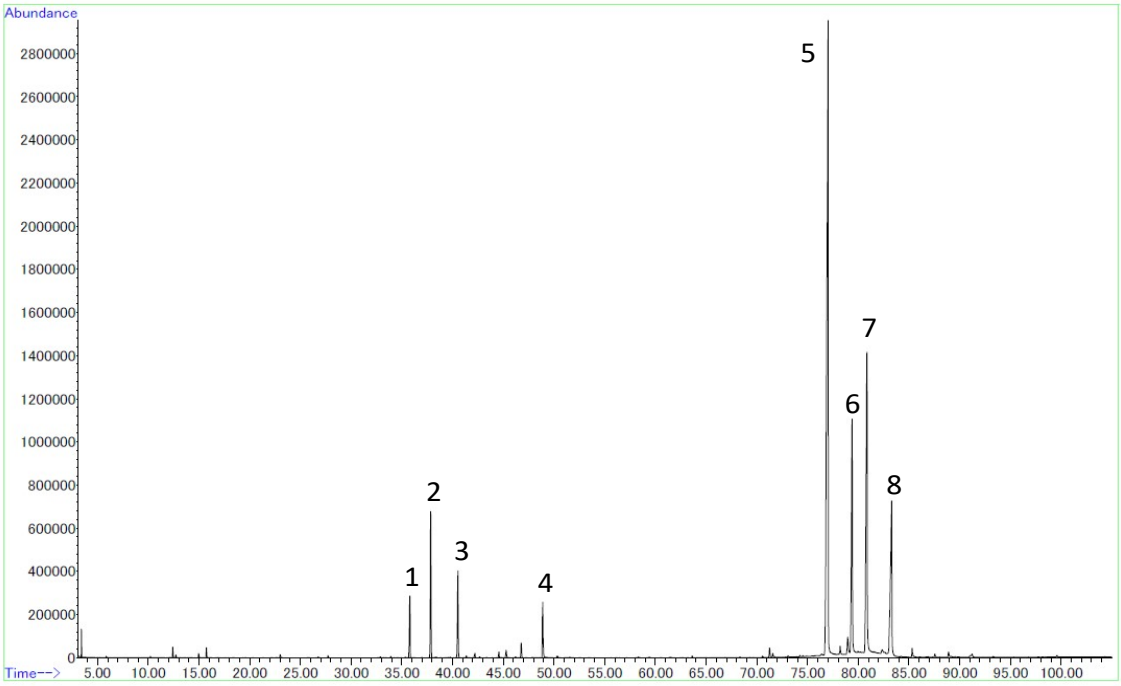

Fig. 2-4. A typical of GC-MS chromatogram of the grains of paradise extract.

Table 2-2. Identified chemical compounds of the grains of paradise extract.

No	Retention time [min]	Compound name	Molecular weight	Characteristic ions [m/z]
1	35.79	Caryophyllene	204.35	204.0, 133.1, 93.1
2	37.86	α-Caryophyllene	204.35	204.2, 121.1, 93.1
3	40.53	β-Chamigrene	204.35	204.2, 189.1, 93.1
4	48.90	Unknown	-	-
5	76.40	[0]-Paradol	194.23	194.0, 137.1, 179.1
6	79.40	[0]-Paradol	194.23	194.0, 137.1, 205.1
7	80.86	*p*-Ethylguaiacol	152.19	152.0, 180.0, 292.2
8	83.30	[0]-Paradol	194.23	194.0, 137.1, 294.2

Generally, in extraction process of plant biomass components including $SCCO_2$ extraction process, the extracted components from the plant biomass matrix could be used as a critical indicator to evaluate an extraction method. This is because of the extracted components allows to represent the components obtained from plant biomass matrix by the particular extraction method. In order to understand the chemical compounds in the extract from grains of paradise seeds by $SCCO_2$ extraction process, the extract was identified by using GC–MS. Next, the identified components of the main peaks in the GC–MS spectra were carried out by using a NIST mass spectral database. **Figure 2-4** showed the GC–MS chromatogram of the compound obtained from grains of paradise seeds when the $SCCO_2$ extraction process was conducted at temperature of 40 ^{o}C and pressure of 20 MPa with 15 min extraction time. The list of identified chemical compounds was showed in the **Table 2-2**. The GC–MS allows to trace a number of small features indicating the presence of lower and higher molecular weight products that varied as a function of temperature. The identities of compounds determined via a match of mass spectra in the GC–MS computer library are reliable. As shown in the **Fig. 2-4**, the compounds such as caryophyllene, α–caryophyllene, β–chamigrene, *p*–ethylguaiacol, and [0]–paradol were detected clearly. However, gingerol and shogaol as major compounds in grains of paradise seeds [23] were not detected due to the prolonged GC–MS analysis at high temperatures. Fernandez *et al.* 2006 [24] reported that due to thermal instability of gingerol and its derived compounds, these compounds were very rarely detected by GC–MS. The degradation of them might be occurred at the instrument

injector port of GC–MS. Sonale and Kadimi 2014 [17] informed that shogaols and paradols were acquired from gingerols during thermal processing, thus they were not found in the fresh of Zingiberaceae species. Shogaols were gingerol analogues with a 4, 5 double bond, generating from elimination of 5–hydroxy groups; and the hydrogenation of shogaol may produce paradol compounds. They also informed that gingerols, shogaols, and paradols which found in the species of Zingiberaceae were homologous series of phenolic ketones and paradols was more stable than gingerols and shogaols. Hence, only paradol compounds were identified by GC–MS.

In order to quantify the amount of gingerol (6–gingerol), shogaol (6–shogaol), and paradol (6–paradol) in the extracts, they were analyzed by high–performance liquid chromatography (HPLC). **Fig. 2-5** showed the HPLC chromatograms of extract grains of paradise seeds by $SCCO_2$ when the extraction was conducted at temperature of 80 ^{o}C and pressure of 20 MPa. There are many grains of paradise seeds components could be extracted from grains of paradise seeds sample. However, in this work, gingerol, shogaol, and paradol were subjected as target compounds and would be determined quantitatively. Gingerol, shogaol, and paradol in the extracts which trapped in 10 ml of ethanol were filtered using a disposable filter of 0.45 μm pore size prior to HPLC analysis. Then, they were directly injected into HPLC equipment. Initially, the pure compound of gingerol or shogaol or paradol diluted in ethanol as a standard was injected in the HPLC system to make calibration curve in 5 point. Next, the amount of each standard leaving the

HPLC column will assign the intensity of the signal generated in the detector. By comparing the time it takes for the peak to show up (the retention time) with the retention times for the standard, the amount of gingerol or shogaol or paradol in the extract can be quantified. This analysis can be performed with good precision; therefore, other methods analysis was not carried out.

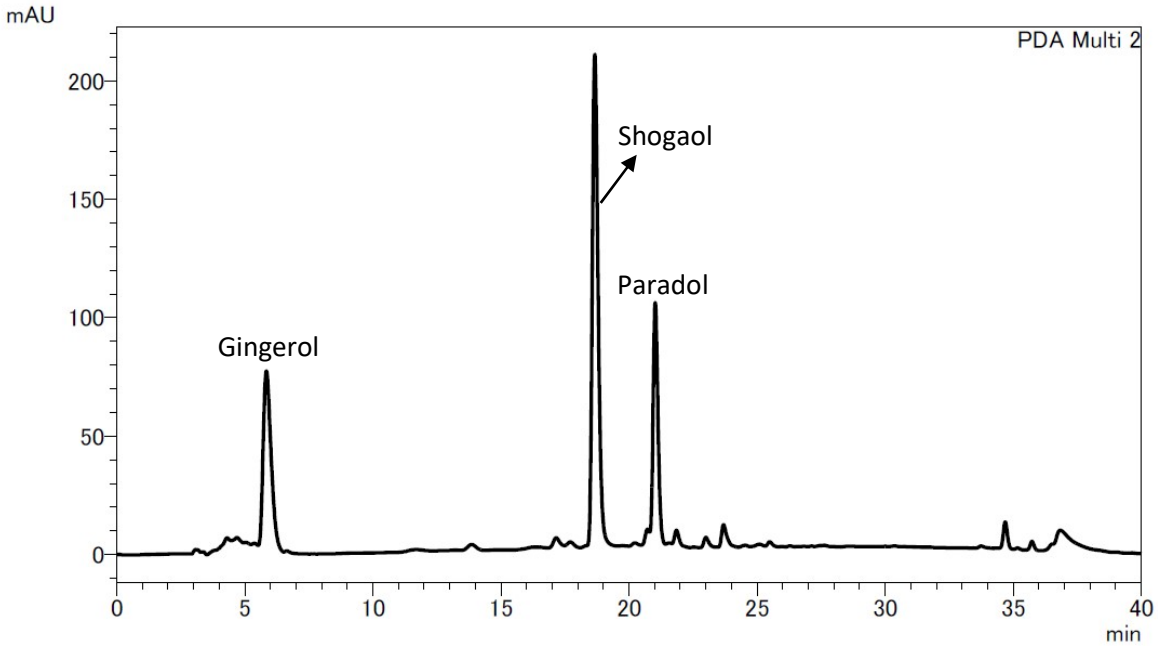

Fig. 2-5. HPLC chromatogram of extracted compounds.

Fig. 2-6 showed the amount of extracts from grains of paradise seeds at various extraction conditions. Obviously, the yields of gingerol, shogaol and paradol differ at different conditions. **Fig. 2-6(a)** shows the influences of extraction pressures on the yields of gingerol, shogaol and paradol at temperature of 80 ^{o}C. The yields of them increased clearly with increasing extraction pressures. At 20 MPa, the yields of gingerol, shogaol and paradol are 1.66, 1.07, and 1.39 mg/g sample, respectively. They increase significantly to 8.12, 3.74, and 3.93 mg/g sample when the extraction pressure is increased to 30 MPa. These results might be related to the density of CO_2 that affect to solubility and dissolution capacity of $SCCO_2$, where, increasing of CO_2 density allows the increasing of extract yields [25–27]. The density of CO2 was 0.59 g/cm^3 at 80 ^{o}C and 20 MPa, then it increased to 0.75 g/cm^3 at 30 MPa with the same temperature. It was clearly that the density of CO_2 can be significantly increased by increasing pressure at a constant temperature lead to an increase in the dissolving capacity of $SCCO_2$ and gives in a beneficial effect on the extraction process. Shi *et al.* 2009 [26] studied the effects of pressure and temperature on the solubility of lycopene in $SCCO_2$ media. They concluded that increasing the CO_2 density at a constant temperature showed a distinct increase in solubility. However, a higher solvation power at higher pressure of $SCCO_2$ (40 MPa) may be associated with lower selectivity [25,28].

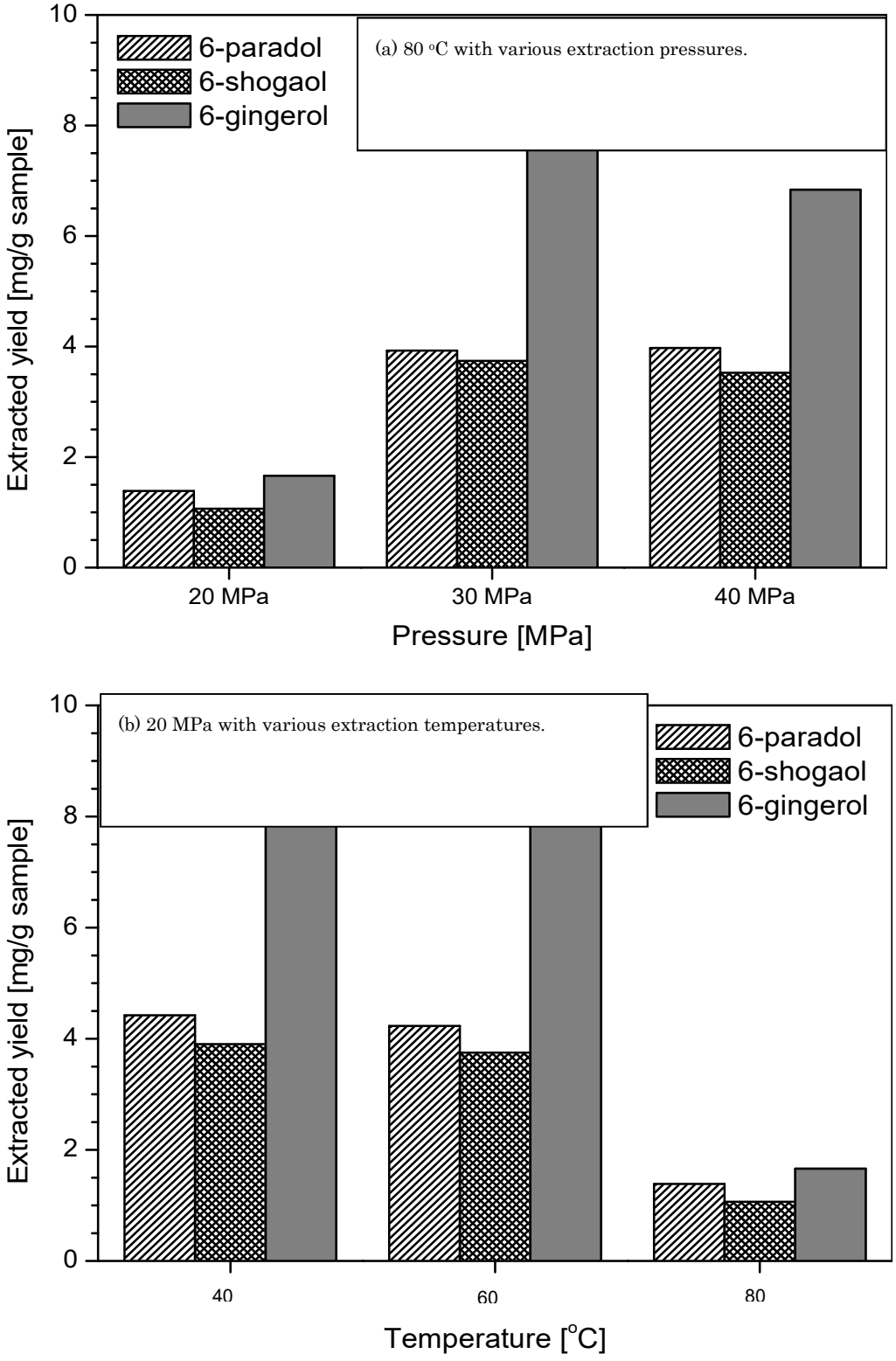

Fig. 2-6. Yields of gingerol, shogaol, and paradol at various extraction conditions.

At higher densities, the $SCCO_2$ is able to contact more surface area, thus resulting more grains of paradise seeds substances to dissolve and be extracted. Consequently, the yields of gingerol, shogaol and paradol seem constant or slightly decrease when the density of CO_2 increases to 0.82 g/cm^3. They are 6.84, 3.53, and 3.97 mg/g sample, respectively. Peterson *et al.* 2006 [28] investigated the supercritical fluid extraction of geranium essential oil from geranium using $SCCO_2$ media at temperatures of 40 – 70 ^oC and pressures of 10 – 30 MPa. They informed that the decreasing extraction yield with increasing pressure is explained in terms of competition between solvent density and solute vapor pressure. At these conditions the change in solvent density becomes smaller and the change in solute vapor pressure becomes more effective and can easily overcome the effect of solvent density change on the extraction yield.

Despite, the density has high effect on the solvent power of $SCCO_2$ media, the ability of $SCCO_2$ solvent extracting also increases with density increase at a certain temperature, or increases with temperature elevate at a certain density [25]. Reverchon and De Marco 2006 [25] explained that extraction pressure is the most important parameter that affects the selectivity and solvent power of $SCCO_2$ extraction media which in turn determine the yield of the target substance. However, they also reported that extraction temperature is also the key parameter in the $SCCO_2$ extraction of substances from various matrices. **Fig. 2-6(b)** shows the effects of extraction

temperatures on the yields of gingerol, shogaol and paradol at pressure of 20 MPa. They decreased clearly with increasing extraction temperatures. At 40 ^{o}C, the yields of gingerol, shogaol and paradol are 9.12, 3.90, and 4.42 mg/g sample, respectively. At 80 ^{o}C, they decreased significantly to 1.66, 1.07, and 1.39 mg/g sample, respectively. Again, these results also might be attributed to the density of CO_2 as an extraction solvent, where, increasing extraction temperatures at the same extraction pressure follow by decreasing of CO_2 density. Consequently, the ability of $SCCO_2$ to extract substances from grains of paradise seeds decreases. Similar results were also reported by Machmudah *et al.* 2012 [29]. They studied the effect of $SCCO_2$ extraction temperature on the β–carotene recovery extracted from tomato peel by–product. The results showed that β–carotene recovery decreased with increasing extraction temperature at a constant pressure. Ghoreishi *et al.* 2012 [30] informed that the effect of extraction temperature in $SCCO_2$ extraction system is more complex due to the competition of two variables, solvent density and vapor pressure. The decrease in solvent density may reduce the solute solubility, while the vapor pressure of the solute elevates with temperature, causing an increase in solubility. The dominant effects of them affected by the system that used as an extraction process. In this study, the effect of CO_2 density seems to have a high effect on the extraction yield.

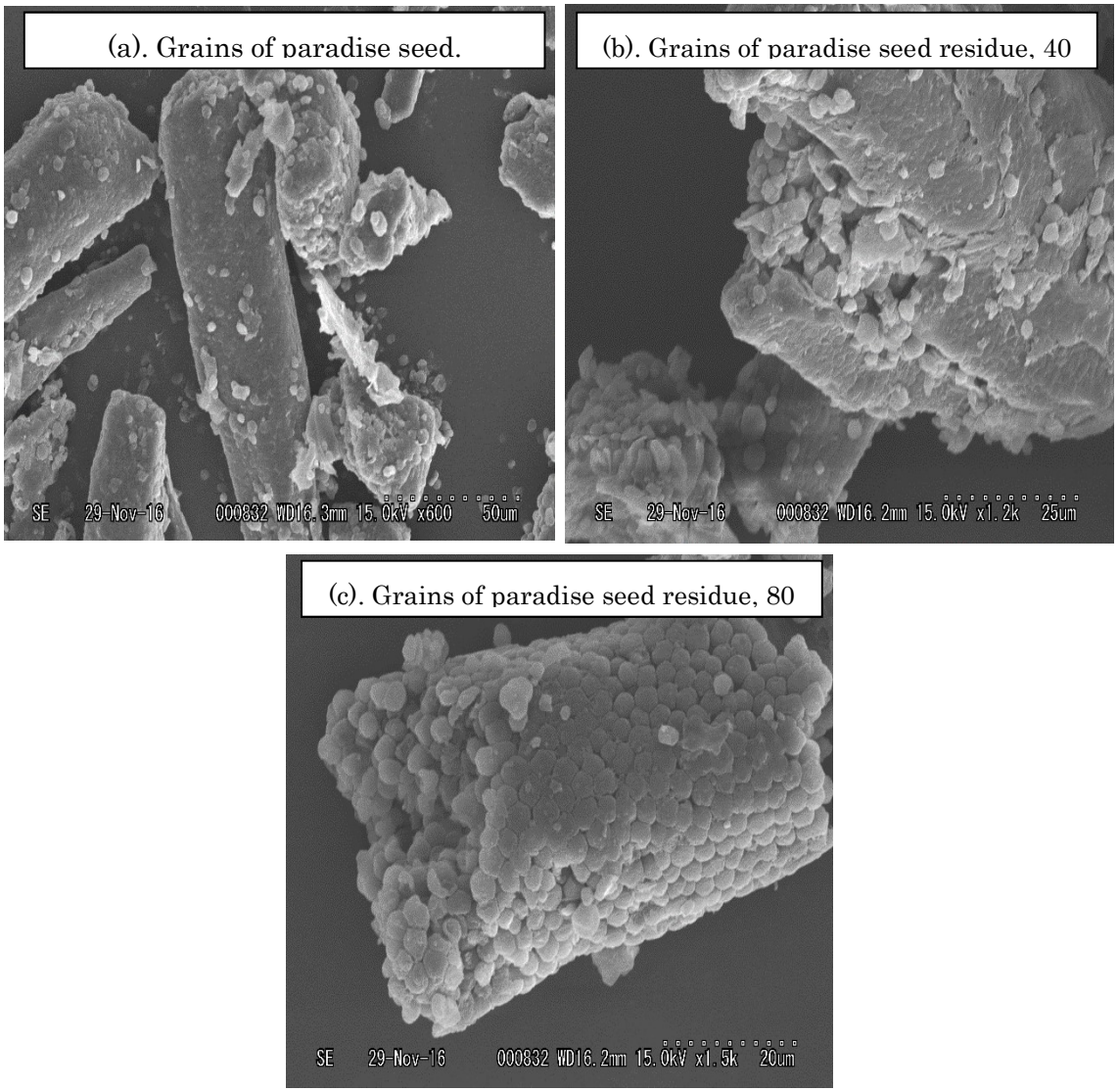

Fig. 2-7. SEM micrographs of grains of paradise seeds before and after treatment by $SCCO_2$.

When a plant matrix is placed in the organic solvent, a static film of solvent surrounding the plant cell would be generated as a result of the interactions between solvent molecules and the plant matrix cell wall substances [31]. Next, the organic solvent diffuses via the cell membrane into the plant matrix cell to form the complexes of organic solvent-plant matrix

substances. As a result, the plant matrix substances might be extracted from the plant matrix cell and remain dissolved in the organic solvent. Similar phenomenon may occur when $SCCO_2$ was contacted with grains of paradise seeds. Here, $SCCO_2$ was flowed via high pressure pump into the extractor from the bottom and passes upwards through the grains of paradise seeds packed bed. At these conditions, $SCCO_2$ rapidly diffuses into the grains of paradise cell and then $SCCO_2$ may dissolve grains of paradise seeds substances via the formation of grains of paradise seeds substance–CO_2 complexes through van der Waals interactions [31]. Due to this interaction, when the $SCCO_2$ leaves the grains of paradise seeds packed bed, the grains of paradise seeds substances might be also left this packed bed simultaneously. In the next process, when the extraction pressure was reduced until CO_2 returns to the gaseous state, the grains of paradise seeds substances extract may be collected and dissolved in ethanol as a trapped solvent in the sample collection. To investigate the effect of $SCCO_2$ that penetrates in grains of paradise seeds, the grains of paradise seeds residues were characterized by SEM. **Fig. 2-7** shows the representative SEM micrographs of grains of paradise seeds before and after $SCCO_2$ extraction treatment. Clearly, the different of surface structures of the grains of paradise seeds before and after $SCCO_2$ extraction treatment were found. Before $SCCO_2$ extraction treatment, the surface morphology of grains of paradise seeds seem covered by the membrane-like structure. Therefore, they were smooth and tight with some boundary edges clearly. They did not exhibit the presence of any pores or surface cracks. After treatment by $SCCO_2$ extraction, the

physical structures disruption of the grains of paradise seeds were found and clearly observed at each condition. Apparently, $SCCO_2$ may rupture the physical structural barriers of the grains of paradise seeds and remove their components. The increasing pressure and temperature (**Fig. 2-7**(c)) seem to an increase of CO_2 diffusivity into the grains of paradise seeds and allow a more powerful swelling action to remove the substances in grains of paradise seeds [21]. Sovova 1994 [32] reported that $SCCO_2$ has ability to rupture cells or the outer surface of matrix to access the solute substances. In detail, the $SCCO_2$ extraction mechanism can be divided into three steps controlled by different mass transfer mechanisms [33]. They are a constant extraction rate period, a falling extraction rate period, and the diffusion controlled rate period. These steps were also initiated by the easily accessible covering solute on the external surface of the matrix. Judging these SEM micrographs, it could be said that the physical changes of the grains of paradise seeds surface happened after $SCCO_2$ extraction treatment.

2-4. Conclusions

$SCCO_2$ has been used as a medium for gingerol, shogaol, and paradol extraction grains of paradise seeds at temperatures of 40 – 80 ^oC and pressures of 20 – 40 MPa using a semi-continuous flow-type system. Due to the combination between high diffusivity and high solvent strength of $SCCO_2$ that can be easily adjusted by changing of temperature and/or pressure,

$SCCO_2$ became an attractive extraction medium. FT–IR spectra indicated that $SCCO_2$ can extract the grains of paradise seeds substances. The SEM micrographs also showed that the physical changes of the grains of paradise seeds surface occurred after $SCCO_2$ extraction. The main compounds in extracts were gingerols, shogaols, and paradols. Since these compounds are homologous series of phenolic ketones and paradols was more stable than gingerols and shogaols, the GC–MS may only detect paradol compounds. The yields of gingerols, shogaols, and paradols were affected by extraction temperatures and/or extraction pressures.

References

[1] M.M. Iwu, Handbook of African Medicinal Plants, Second Edition, CRC Press Taylor & Francis Group, New York, 123, (2014)

[2] A. Khoddami, M.A. Wilkes, T.H. Roberts, Techniques for analysis of plant phenolic compounds, *Molecules*, 18, 2, 2328-2375 (2013)

[3] R.Y. Gan, Z.Q. Deng, A.X. Yan, N.P. Shah, W.Y. Lui, C.L. Chan, H. Corke, Pigmented edible bean coats as natural sources of polyphenols with antioxidant and antibacterial effects, *LWT - Food Sci. Technol.*, 73, 168-177 (2016)

[4] X. Fernandez, C. Pintaric, L. Lizzani-Cuvelier, A.M. Loiseau, A. Morello, P. Pellerin, Chemical composition of absolute and supercritical carbon dioxide extract of Aframomum melegueta, *Flavour Frag. J.*, 21, 1, 162-165 (2006)

[5] M. Iwami, F.A. Mahmoud, T. Shiina, H. Hirayama, T. Shima, J. Sugita, Y. Shimizu, Extract of grains of paradise and its active principle 6-paradol trigger thermogenesis of brown adipose tissue in rats, *Auton. Neurosci.*, 161, 1, 63-67 (2011)

[6] Y. Kawamoto, Y. Ueno, E. Nakahashi, M. Obayashi, K. Sugihara, S. Qiao, M. Iida, M.Y. Kumasaka, I. Yajima, Y. Goto, N. Ohgami, M. Kato, K. Takeda K, Prevention of allergic rhinitis by ginger and the molecular basis of immunosuppression by 6-gingerol through T cell inactivation, *J. Nutr. Biochem.*, 27, 112-122 (2016)

[7] S.M. Kim, C. Kim, H. Bae, J.H. Lee, S.H. Baek, D. Nam, W.S. Chung, B.S. Shim, S.G. Lee, S.H. Kim, G. Sethi, K.S. Ahn, 6-Shogaol exerts anti-proliferative and pro-apoptotic effects through the modulation of STAT3 and MAPKs signaling pathways. *Mol. Carcinog.*, 54, 10, 1132-1146 (2015)

[8] A. Saha, J. Blando, E. Silver, L. Beltran, J. Sessler, J. DiGiovanni, 6-Shogaol from dried ginger inhibits growth of prostate cancer cells both in vitro and in vivo through inhibition of STAT3 and NF-κB signaling, *Cancer Prev. Res.*, 7, 6, 627-638 (2014)

[9] Y. Zhou, Q. Tang, S. Zhao, F. Zhang, L. Li, W. Wu, Z. Wang, S. Hann, Targeting signal transducer and activator of transcription 3 contributes to the solamargine-inhibited growth and -induced apoptosis of human lung cancer cells, *Tumor Biol.*, 35, 8, 8169-8178 (2014)

[10] S. Machmudah, A. Shotipruk, M. Goto, M. Sasaki, T. Hirose, Extraction of astaxanthin from *Haematococcus pluvialis* using supercritical CO_2 and ethanol as entrainer, *Ind. Eng. Chem. Res.*, 45, 10, 3652-3657 (2006)

[11] K. Kitada, S. Machmudah, M. Sasaki, M. Goto, Y. Nakashima, S. Kumamoto, and T. Hasegawa, Supercritical CO_2 extraction of pigment 1components with pharmaceutical importance from *Chlorella vulgaris*, *J. Chem. Technol. Biotechnol.*, 84, 5, 657-661 (2009)

[12] D. Ruen-ngam, A. Shotipruk, P. Pavasant, S. Machmudah, M. Goto, Selective extraction of lutein from alcohol treated Chlorella vulgaris by supercritical CO_2, *Chem. Eng. Technol.*, 35, 2, 255-260 (2012)

[13] H. Kanda, Y. Kamo, S. Machmudah, Wahyudiono, M. Goto, Extraction of fucoxanthin from raw macroalgae excluding drying and cell wall disruption by liquefied dimethyl ether, *Mar. Drugs*, 12, 5, 2383-2396 (2014)

[14] M. Goto, H. Kanda, Wahyudiono, S. Machmudah, Extraction of carotenoids and lipids from algae by supercritical CO_2 and subcritical dimethyl ether, *J. Supercrit. Fluids*, 96, 245-251 (2015)

[15] S. Machmudah, T. Izumi, M. Sasaki, M. Goto, Extraction of pungent components from Japanese pepper (*Xanthoxylum piperitum DC.*) using supercritical CO_2, *Sep. Pur. Technol.*, 68, 2, 159-164 (2009)

[16] M.E. Leblebici, S. Machmudah, M. Sasaki, M. Goto, Antiradical Efficiency of Essential Oils from Plant Seeds Obtained by Supercritical CO_2, Soxhlet Extraction, and Hydrodistillation, *Sep. Sci. Technol.*, 48, 2, 328-337 (2012)

[17] R.S. Sonale, U.S Kadimi, Characterization of gingerol analogues in supercritical carbon dioxide (SC CO_2) extract of ginger (*Zingiber officinale,* R.,), *J. Food Sci. Technol.*, 51, 11, 3383-3389 (2014)

[18] S. Machmudah, A. Martin, M. Sasaki, M. Goto, Mathematical modeling for simultaneous extraction and fractionation process of coffee beans with supercritical CO_2 and water, *J. Supercrit. Fluids*, 66, 111-119 (2012)

[19] K. Tomitaa, S. Machmudah, Wahyudiono, R. Fukuzato, H. Kanda, A.T. Quitain, M. Sasaki, M. Goto, Extraction of rice bran oil by supercritical carbon dioxide and solubility consideration, *Sep. Pur. Technol.*, 125, 319-325 (2014)

[20] Y. Matsunaga, Wahyudiono, S. Machmudah, M. Sasaki, M. Goto, Hot compressed water extraction of polysaccharides from *Ganoderma lucidum* using a semibatch reactor, *Asia Pac. J. Chem. Eng.*, 9, 1, 125-133 (2014)

[21] S. Kodama, T. Shoda, S. Machmudah, Wahyudiono, H. Kanda, M. Goto, Enhancing pressurized water extraction of b-glucan from barley grain by adding CO2 under hydrothermal conditions, *Chem. Eng. Process. Process Intensif.*, 97, 45-54 (2015)

[31] R. Halim, M.K. Danquah, P.A. Webley, Extraction of oil from microalgae for biodiesel production: A review, *Biotechnol. Adv.*, 30, 3, 709-732 (2012)

[32] H. Sovova, Rate of the vegetable oil extraction with supercritical CO_2-I. Modelling of extraction curves, *Chem. Eng. Sci.*, 49, 3, 409-414 (1994)

[33] A. Shilpi, U.S. Shivhare, S. Basu, Supercritical CO_2 Extraction of Compounds with Antioxidant Activity from Fruits and Vegetables Waste-A Review, *Focusing on Modern Food Industry*, 2, 1, 43-62 (2013)

Chapter 3

Nanoparticle production of lycopene(SEDS)

3-1. Introduction

The effect of the *Z*-isomer content on particle production of lycopene by the solution-enhanced dispersion by supercritical fluids (SEDS) process was evaluated. Using the thermal isomerization and filtering technique, lycopene containing a large amount of *Z*-isomers (65.3% and 97.8%) was prepared from (all-*E*)-lycopene. When (all-*E*)-lycopene was used as a raw material for SEDS precipitation, particles with an average size of 3.6 μm were obtained. On the other hand, when using lycopene containing a large amount of the *Z*-isomers, the lycopene particles became significantly finer compared with those obtained using (all-*E*)-lycopene. For example, when using lycopene containing 97.8% *Z*-isomers, uniformly sized particles with an average size of 75 nm were obtained. Interestingly, despite the *Z*-isomer content of the raw materials, the obtained lycopene particles were primarily in the thermodynamically stable all-*E* isomer. Therefore, the *Z*-isomerization pre-treatment of lycopene is very effective to obtain uniform, stable, and fine particles using SEDS precipitation.

3-2. Carotenoids

Carotenoids are the most common fat-soluble plant pigments in nature, numbering at more than 750 different types. Lycopene is an acyclic carotenoid containing 11 conjugated double bonds, and is found abundantly in vegetables and fruits with a bright-red color, such as tomatoes and watermelons [1, 2]. In recent years, lycopene has attracted more and more attention because of its potential anticancer and antiarteriosclerotic actions, as well as its strong antioxidant properties [3–5]. Numerous studies have demonstrated that micronization effectively enhances the bioavailability of carotenoids [6, 7]. However, there are some concerns over conventional particle micronization methods such as grinding, milling, spray drying, and chemical precipitation. Carotenoids treated by mechanical processes could be degraded by oxygen contact and friction heat. Furthermore, those treated by chemical processes may contain toxic organic solvent residues. To obtain fine particles, the use of supercritical carbon dioxide ($SCCO_2$) has attracted attention. Since CO_2 has a low critical temperature (T_c = 31.1 °C), it is suitable for heat-sensitive materials, and $SCCO_2$ is non-toxic and easily separated from the products along with the organic solvent. Among several particle micronization techniques using supercritical fluids, supercritical anti-solvent (SAS) micronization has been widely studied as an effective and simple method to make fine particles from various materials such as pharmaceutical compounds and pigments [8–11]. In this study, the micronization of lycopene

was conducted using solution-enhanced dispersion by supercritical fluids (SEDS), which is a modified version of the SAS process [10–12]. In this process, the solution and $SCCO_2$ are sprayed into a precipitator by a coaxial nozzle.

Carotenoids in plants are accumulated predominantly as the (all-*E*)-configuration and have higher crystallizability [13]. Thus, it is difficult to produce nano-sized particles, which improves the bioavailability, by chemical and physical micronization methods of (all-*E*)-lycopene [8–11]. For example, Miguel et al. [8] conducted micronization of lycopene using SAS preparation under various conditions, but it was impossible to obtain lycopene having particles of submicron or finer sizes. There is limited evidence that the physical properties of carotenoids may change by *Z*-isomerization [13–15], e.g., Murakami et al. [13] found that, as the *Z*-isomer content of lycopene increased, its solubility increased significantly and it changed from the crystalline to an amorphous state. Thus, since the *E* and *Z* forms of lycopene have significantly different physical properties, the efficiency of micronization is also expected to be greatly different. Here, we report the first instance of the effect of the *Z*-isomer content on nanoparticle production of a carotenoid, lycopene, using the SEDS process, and revealed that as the *Z*-isomer content increased, the particle sizes became smaller. This new finding is an effective tool for the micronization of carotenoids with high safety and will contribute to the understanding of characteristics of *Z*-isomers of carotenoids.

3-3. Materials and methods

3-3-1. Chemicals

High-performance liquid chromatography (HPLC)-grade ethyl acetate and hexane were purchased from Wako Pure Chemical Industries, Ltd. (Osaka, Japan). *N*,*N*-Diisopropylethylamine (DIPEA) was obtained from Tokyo Chemical Industry Co., Ltd. (Tokyo, Japan).

3-3-2. Preparation of (all-E)-lycopene

High purity (all-*E*)-lycopene was obtained from tomato oleoresin (Lyc-O-Mato 15%, LycoRed Ltd., Beer-Sheva, Israel) according to the previous method with some modifications [16]. Briefly, 5.0 g of the oleoresin was dissolved in 150 mL of benzene by sonication for 10 min. The insoluble substances were collected by suction filtration on a Kiriyama funnel (number 5B filter paper), and the residue was rinsed with 100 mL of benzene. The obtained red solid on the filter was dissolved in 50 mL of acetone by sonication for 10 min, and insoluble substances were collected by suction filtration. The residue was rinsed sequentially with 100 mL of acetone, 150 mL of ethanol, and 100 mL of hexane, and dried *in vacuo*, yielding 437 mg of fine red crystalline (all-*E*)-lycopene (normal-phase HPLC, ≥98.0% purity).

3-3-3. Preparation of Z-isomers of lycopene

Lycopene containing a large amount of *Z*-isomers was prepared by the thermal isomerization and filtering technique from purified (all-*E*)-lycopene described previously [17, 18]. Briefly, (all-*E*)-lycopene was dissolved in dichloromethane (CH_2Cl_2) at a concentration of 1 mg/mL and heated at 80 °C for 8 h. The lycopene solution was evaporated to dryness under reduced pressure at 40 °C and the residue (ca. 50 mg) was suspended in 10 mL of ethanol. The insoluble substances, mostly consisting of (all-*E*)-lycopene, were removed using a 0.2-μm membrane filter (DISMIC-25HP, Advantec, Tokyo), and ethanol was removed under reduced pressure at 40 °C. In this study, purified (all-*E*)-lycopene, thermally *Z*-isomerized lycopene, and the filtered lycopene were used as raw materials for micronization by the SEDS process. Before the process, the raw materials were dissolved in ethyl acetate, all at a concentration of 0.1 mg/mL.

3-3-4. Particle formation by SEDS process

A schematic diagram of the SEDS micronization of lycopene is shown in **Fig. 3-1**. The apparatus includes a chiller (CCA-1111, Tokyo Rikakikai Co., Ltd., Tokyo), two high-pressure pumps, one for CO_2 (PU–2086, Jasco Co.,

Tokyo) and the other for the lycopene solution (LC–20AT, Shimadzu Co., Ltd., Kyoto, Japan), a heating chamber (EI-700B, As One Co., Osaka, Japan), a coaxial nozzle (**Fig. 3-1**, nozzle inner diameters 2.4 and 0.8 mm, inner diameter of the nozzle outlet 0.4 mm, custom-made by Taiatsu Techno Co., Tokyo), a membrane filter for collecting particles (100 nm PTFE membrane filter, Advantec Co., Ltd., Tokyo) placed inside a Swagelok filter housing, a back pressure regulator (BPR; Akico Co., Ltd., Tokyo), and a wet gas meter (Shinagawa Co., Ltd., Tokyo).

The micronization of lycopene using the above apparatus was carried out according to the following procedures [9–11]. Supercritical CO_2 was flowed to the nozzle at a flow rate of 15 mL/min until the temperature and pressure reached 40 °C and 10 MPa, respectively. The lycopene solution in ethyl acetate was pumped at a flow rate of 0.5 mL/min for 3 h. After the micronization process was completed, the flow of the lycopene solution was stopped but the flow of CO_2 was continued for an additional 30 min to ensure that all the residual solvent was removed from the lycopene particles. Finally, the lycopene particles were collected from the membrane filter after depressurization.

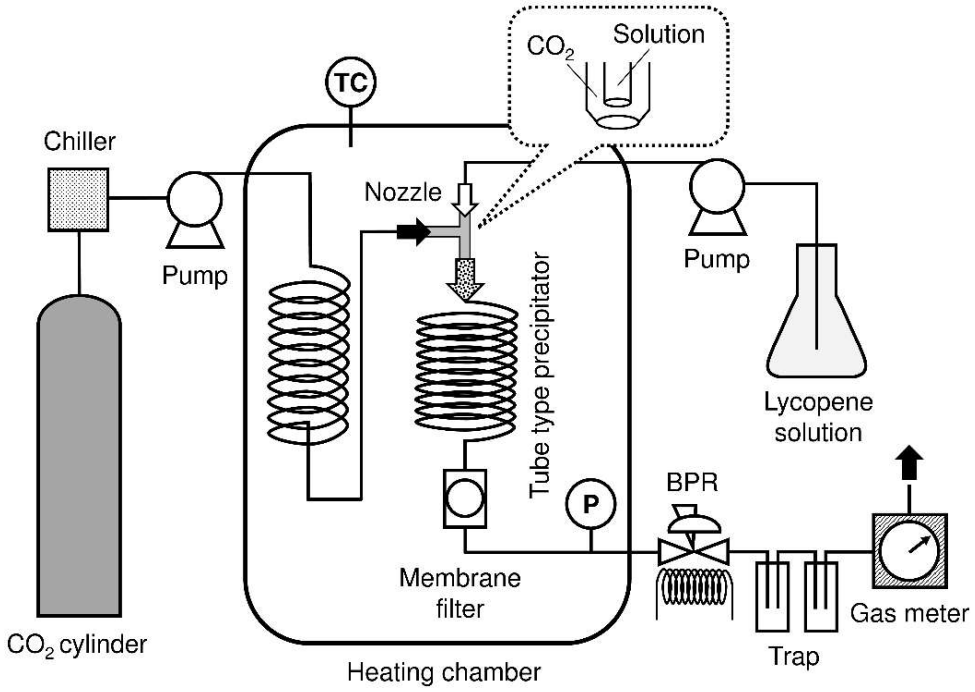

Fig. 3-1. Schematic diagram of the SEDS process.

3-3-5. HPLC analysis

Normal-phase HPLC analysis with a photodiode array detector (MD-2010 Plus, Jasco Co., Ltd., Tokyo, Japan) was conducted according to the method described previously [16]. The analysis was performed on three Nucleosil 300-5 columns connected in tandem (4 × 250 mm in length, 4.6-mm inner diameter, 5-μm particle size; GL Sciences Inc., Tokyo, Japan) with

hexane containing 0.075% DIPEA, at a flow rate of 1.0 mL/min, and a column temperature of 30 °C. The quantification of lycopene isomers was performed by peak area integration at 460 nm, at which the differences in molar extinction coefficients among lycopene isomers are relatively small [16–18]. Lycopene isomer peaks were identified according to HPLC retention times, visible spectral data, and the relative intensities of the *Z*-peak (% D_B/D_{II}), as described previously [16, 18–20]. The *Z*-isomer content (%) was estimated from the ratio of the total amount of *Z*-isomers to the total amount of all lycopene isomers, including the (all-*E*)-isomer.

3-3-6. SEM analysis

The shape and surface characteristics of the lycopene particles were observed by scanning electron microscopy (SEM; JSM-6390LV JEOL, Tokyo, Japan). The samples were sputter-coated with gold in a high-vacuum evaporator and examined using SEM at 15 kV [13]. Particle sizes and size distributions were measured using Image J software for at least 100 particles collected at each experiment [10].

3-3-7. Powder XRD analysis

XRD measurements of the obtained fine particles of lycopene were performed on a Rigaku FR-E X-ray diffractometer. Cu Kα radiation (λ = 1.542 Å) was used with a beam size of approximately 300 μm × 300 μm, with a camera length of 70 mm. The powder sample was placed in a capillary tube (⌀1.0 mm) and was irradiated with the X-ray beam without further adjustments [13].

3-4. Results and discussion

3-4-1. Profile of thermally Z-isomerized lycopene

Purified (all-*E*)-lycopene dissolved in CH_2Cl_2 isomerized to the *Z*-isomers by heating at 80 °C; the total *Z*-isomer content reached 65.3% after heating for 8 h. Furthermore, by the filtration treatment, the *Z*-isomer content successfully increased to 97.8%. The typical chromatograms of a thermally *Z*-isomerized sample and its filtered sample are shown in **Fig. 3-2**, as well as that of intact (all-*E*)-lycopene. The absorption maxima and the relative intensities of the *Z*-peak (% D_B/D_{II}) for each peak 1–10 in the chromatograms were measured using a photodiode array detector, and some of the peaks were tentatively identified (**Table 3-1**). Upon thermal *Z*-isomerization of (all-*E*)-

lycopene, mainly (5*Z*)-, (9*Z*)-, and (13*Z*)-lycopene emerged, and small amounts of multi-*Z*-isomers, such as (9*Z*,13′*Z*)-, (5*Z*,9*Z*)-, and (5*Z*,5′*Z*)-lycopene, increased. These observations were also described in previous studies [13, 17]. After the filtration of thermally *Z*-isomerized lycopene dissolved in ethanol, the content of (all-*E*)-lycopene and (5*Z*)-lycopene significantly decreased (**Fig. 3-2C**), and thus the total *Z*-isomer content increased. This is an indication that those isomers have low solubility in ethanol. Next, the micronization efficiencies of (all-*E*)-lycopene and lycopene containing 65.3% and 97.8% *Z*-isomers using SEDS precipitation were compared.Some of the peaks (1–10) were tentatively identified as shown in **Table 3 -1**.

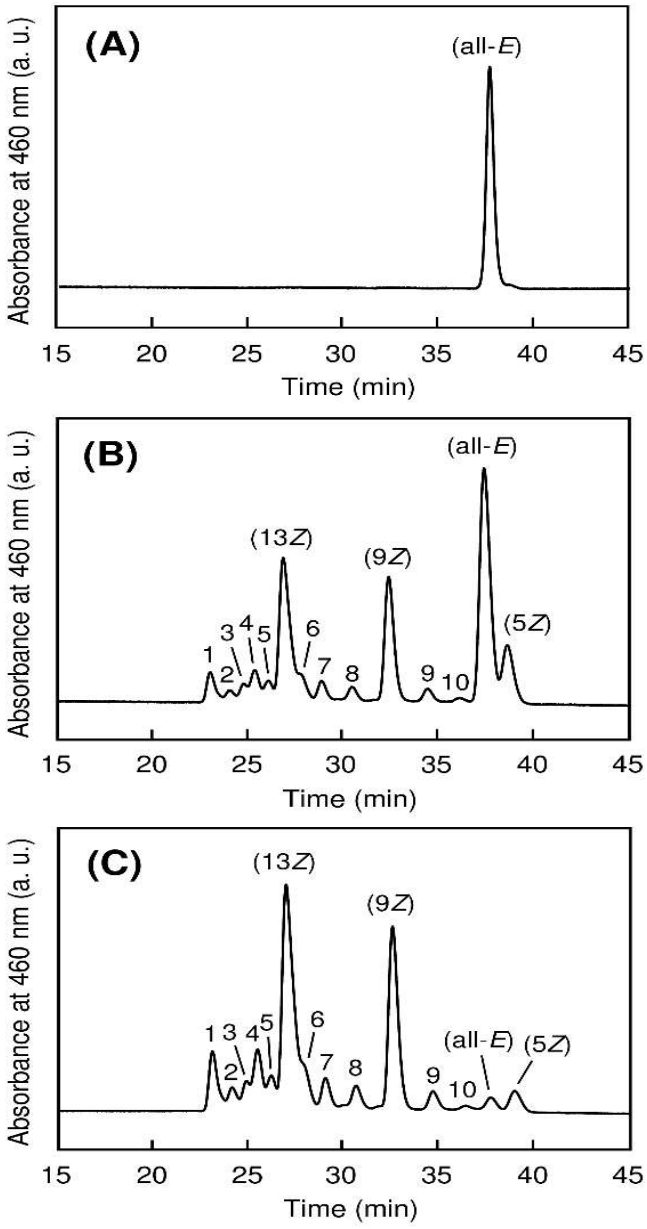

Fig. 3-2. Normal-phase HPLC chromatograms of (A) purified (all-*E*)-lycopene, (B) thermally treated lycopene at 80 °C for 8 h, and (C) filtered lycopene. (5*Z*)-, (9*Z*)-, and (13*Z*)-Lycopene designated in the chromatograms were identified according to previous studies [16, 18–20].

Table 3-1
Absorption maxima (λ_{max}) and relative intensities of the *Z*-peak (%D_B/D_{II}) for geometrical lycopene isomers separated and observed using normal-phase high-performance liquid chromatography.[a]

Peak	Lycopene isomer[b]	λ_{max} (nm)		% D_B/D_{II}	
		In-line	Reported[b]	In-line	Reported[b]
1	(9Z,13′Z)	359, 431, 455, 487	360, 433, 457, 487	30.6	30.4
2	(9Z,9′Z)	359, 431, 459, 487	360, 433, 459, 490	10.2	9.5
3	UZ	359, 435, 463, 491	–	53.1	–
4	UZ	359, 431, 455, 487	–	24.3	–
5	UZ	359, 435, 463, 495	–	55.8	–
	(13Z)	359, 435, 463, 491	361, 437, 463, 494	54.4	52.4
6	UZ	359, 443, 463, 495	–	56.2	
7	(5Z,9′Z)	359, 435, 463, 495	361, 438, 464, 495	13.7	13.4
8	UZ	359, 431, 455, 483	–	12.5	–
	(9Z)	359, 435, 463, 495	361, 438, 464, 495	13.0	12.7
9	(5Z,9Z)	359, 439, 463, 495	361, 438, 464, 495	7.2	11.8
10	(5Z,5′Z)	443, 471, 499	443, 470, 502	ND	ND
	(all-*E*)	443, 471, 499	444, 470, 502	ND	ND
	(5Z)	443, 471, 499	444, 470, 502	ND	ND

[a] Values and peak designations were obtained from the chromatograms in Fig. 1. UZ, unidentified *Z*-isomer of lycopene. –, not assigned. ND, not detected substantially.
[b] Tentatively assigned by the literature [16, 18–20].

3-4-2. Particle formation by SEDS process

Fig. 3-3 shows SEM images of lycopene particles after the SEDS process, and **Fig. 3-4** shows the particle size distributions of the treated particles. As with previous studies [8, 10], when purified (all-*E*)-lycopene was used as the raw material, the obtained lycopene powder exhibited flake-shaped crystals with a mean diameter of 3.6 µm. When the lycopene contained 63.5% *Z*-isomers, the lycopene particles became smaller as a whole compared with (all-*E*)-lycopene, and both flake-shaped crystals and spherical particles with a mean diameter of 0.8 µm were observed. Moreover, when the lycopene

contained 97.8% *Z*-isomers, most lycopene particles existed as uniform spherical particles with a mean diameter of 75 nm. Miguel et al. [8] carried out the micronization of crystalline lycopene (all-*E* form) by SAS preparation under various conditions, and found that the particle size decreased with the pressure reduction in the range of 9–15 MPa. However, when treated at 9 MPa, the mean particle size was about 10 μm, and it was impossible to achieve submicron or finer sizes for which the improvement of bioavailability has been confirmed [6, 7]. On the other hand, Nerome et al. [10] successfully prepared 40 nm lycopene particles using the SEDS process. However, they used β-cyclodextrin as a complex, and in the case of lycopene only, micronization products of less than submicron size could not be achieved. Therefore, the *Z*-isomerization pre-treatment is very effective in forming nanoparticles of lycopene. Even in carotenoids other than lycopene such as β-carotene and zeaxanthin, the physical properties change by *Z*-isomerization [15, 21]. Therefore, the *Z*-isomerization treatment before the SEDS process is highly likely to be effective for all carotenoids.

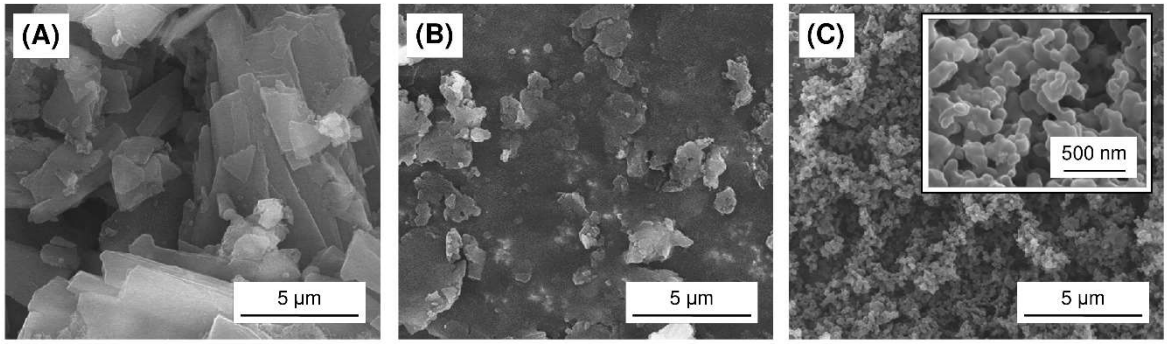

Fig. 3-3. SEM images of lycopene particles after the SEDS process: (A) purified (all-*E*)-lycopene; (B) thermally treated lycopene at 80 °C for 8 h; (C) filtered lycopene.

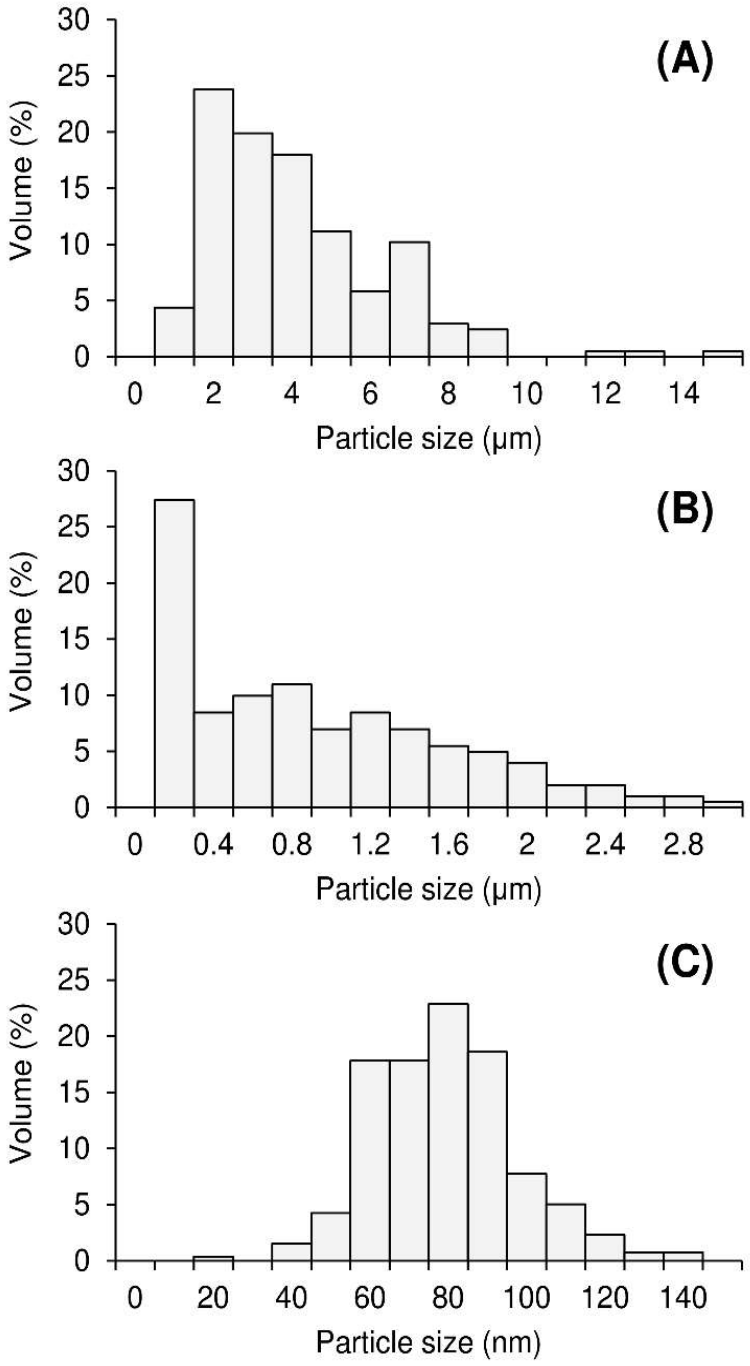

Fig. 3-4. Particle size distributions of lycopene particles after SEDS process: (A) purified (all-*E*)-lycopene; (B) thermally treated lycopene at 80 °C for 8 h; (C) filtered lycopene.

Typical HPLC chromatograms of obtained lycopene particles are shown in **Fig. 3-5**. Interestingly, the *Z*-isomer content of the particles using lycopene containing 63.5% and 97.8% *Z*-isomers as raw materials were only 6.0% and 10.9%, respectively. This indicated that the particles consisted of mainly (all-*E*)-lycopene. In addition, when using lycopene containing 97.8% *Z*-isomers, the recovery (wt%: the amount of lycopene trapped by the 100 nm membrane filter to the amount of the lycopene raw material) was 22.2% (For reference, when using (all-*E*)-lycopene, the recovery was 84.4%). Thus, considering the mass balance, some *Z*-isomers isomerized to the (all-*E*)-isomer during the SEDS process. Christoph et al. [22] reported that when lycopene was heated in solvents having a low solubility for lycopene, the *Z*-isomers easily isomerized to the (all-*E*)-isomer. In addition, several studies have reported that the all-*E* isomer is the most thermodynamically stable of the lycopene isomers [18, 23]. Lycopene passed through the filter was recovered in the trap after BPR (**Fig. 3-1**), and the total *Z*-isomer content was found to be 86.5% (**Fig. 3-6**). This indicated that the *Z*-isomers of the lycopene particles were too small to be trapped by the filter and/or the *Z*-isomers have higher solubility in $SCCO_2$ [24, 25] and thus passed through the filter without forming particles (which of the two is the cause is unclear in this study.). From the above, it can be guessed that the *Z*-isomers of lycopene isomerized to the all-*E* form during the SEDS process, and (all-*E*)-lycopene formed the particles. However, since the content of the *Z*-isomers in the $SCCO_2$ was high, crystal growth was inhibited. That is why, when lycopene containing a large amount of *Z*-isomers was used as the raw material in the SEDS

process, the obtained particles became smaller and mainly consisted of the all-*E* isomer.

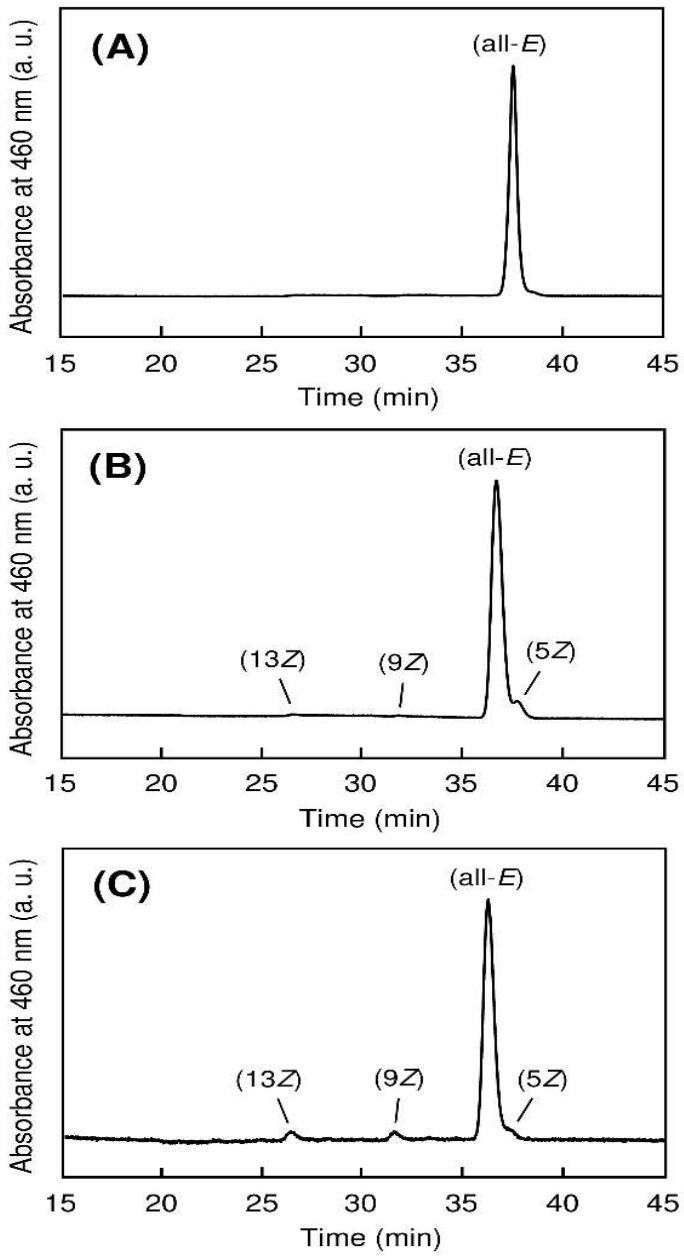

Fig. 3-5. Normal-phase HPLC chromatograms of lycopene particles obtained by the SEDS precipitation from (A) purified (all-*E*)-lycopene, (B) thermally treated lycopene at 80 °C for 8 h, and (C) filtered lycopene. (5*Z*)-, (9*Z*)-, and (13*Z*)-Lycopene designated in the chromatograms were identified according to previous studies [16, 18–20].

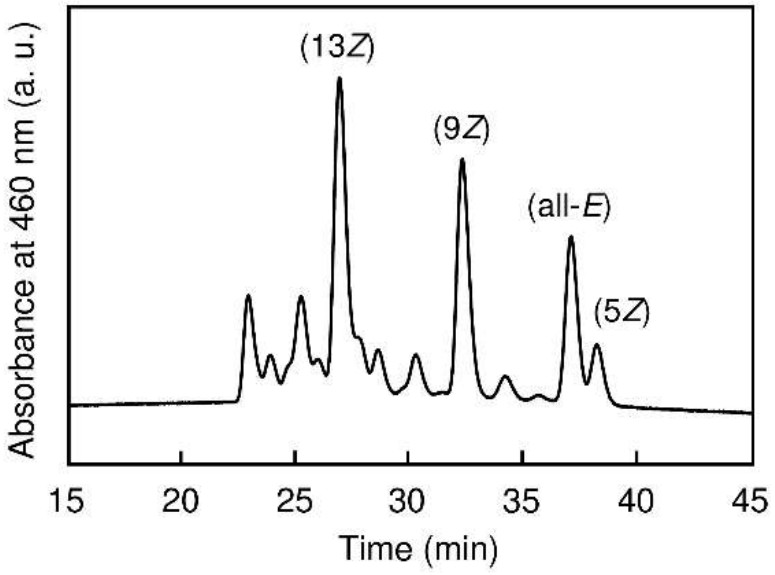

Fig.3-6. Normal-phase HPLC chromatogram of lycopene which was recovered in the trap after BPR (Fig. 1). (5*Z*)-, (9*Z*)-, and (13*Z*)-Lycopene designated in the chromatogram were identified according to previous studies [16, 18–20].

Fig. 3-7 shows powder XRD patterns of the lycopene particles after the SEDS process. When purified (all-*E*)-lycopene was used as the raw material, sharp and clear peaks were observed at a diffraction angle 2θ value of 5–30° and the pattern was similar to that of crystalline lycopene (all-*E*-form) reported previously [13, 26]. On the other hand, when lycopene containing 63.5% and 97.8% *Z*-isomers was used as the raw material, those peaks became smaller and the number of peaks decreased even though the obtained particles contained a large amount of (all-*E*)-lycopene. This was due to the

reduction of the lycopene particle size [27] and the presence of a small amount of the *Z*-isomers (**Fig. 3-5B and C**) [13]. (all-*E*)-Carotenoid molecules can be stabilized via π-π stacking interactions of conjugated polyene chains, and thus carotenoids have high crystalline properties. However, upon increasing the *Z*-isomer content, enormous steric hindrance occurs, diminishing the potential attractive forces, resulting in the decrease of crystallinity [15]. In fact, Murakami et al. [13] demonstrated by powder XRD analysis that as the lycopene *Z*-isomer content increased, the peaks originating from lycopene became smaller and the number of peaks decreased. Therefore, it is considered that when lycopene containing a large amount of the *Z*-isomers was used as a raw material in SEDS precipitation, the *Z*-isomers were included in the obtained particles, which markedly lowered the crystallinity of lycopene.

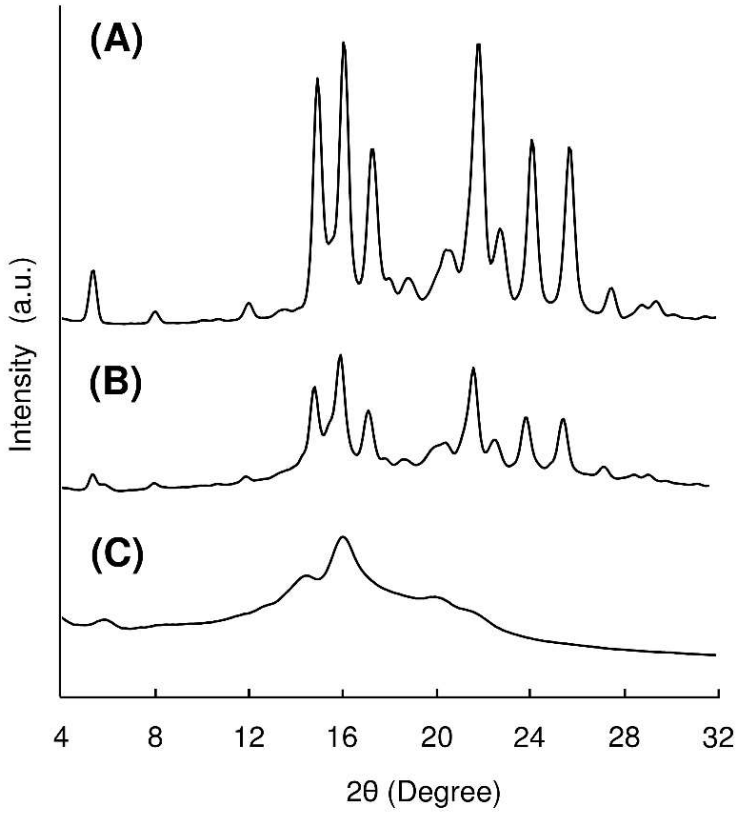

Fig. 3-7. Powder XRD patterns of lycopene particles after the SEDS process: (A) purified (all-*E*)-lycopene; (B) thermally treated lycopene at 80 °C for 8 h; (C) filtered lycopene.

3-5. Conclusion

The effect of the *Z*-isomer content on micronization of lycopene by the SEDS process was investigated. As the *Z*-isomer content increased, the particle sizes became smaller and, despite the lycopene *Z*-isomer content of

the raw material, the obtained lycopene particles were mainly the all-*E* form. These results indicated that some *Z*-isomers of lycopene isomerized to the all-*E* isomer in the SEDS process, and while the all-*E* isomer could form large lycopene particles, the presence of the *Z*-isomers inhibited crystal growth. Since most lycopene *Z*-isomers passed through the 100 nm PTFE membrane filter, they either formed very small particles that could easily pass through the filter and/or remained dissolved in $SCCO_2$ because they have higher solubility.

References

[1] H. Aoki, N.T. Kieu, N. Kuze, K. Tomisaka, N. Van Chuyen, Carotenoid pigments in GAC fruit (*Momordica cochinchinensis* SPRENG), *Biosci. Biotechnol. Biochem*. 66, 2479–2482 (2002)

[2] J.M. Holden, A.L. Eldridge, G.R. Beecher, I.M. Buzzard, S. Bhagwat, C.S. Davis, L.W. Douglass, S. Gebhardt, D. Haytowitz, S. Schakel, Carotenoid content of U.S. foods: an update of the database, *J. Food Compos. Anal*. 12, 169–196 (1999)

[3] K. Ried, P. Fakler, Protective effect of lycopene on serum cholesterol and blood pressure: Meta-analyses of intervention trials, *Maturitas* 68, 299−310 (2011)

[4] K. Dahan, M. Fennal, N.B. Kumar, Lycopene in the prevention of prostate cancer, *J. Soc. Integr. Oncol*. 6, 29−36 (2008)

[5] A. Ouchi, K. Aizawa, Y. Iwasaki, T. Inakuma, J. Terao, S. Nagaoka, K. Mukai, Kinetic study of the quenching reaction of singlet oxygen by carotenoids and food extracts in solution. Development of a singlet oxygen absorption capacity (SOAC) assay method, *J. Agric. Food Chem*. 58, 9967−9978 (2010)

[6] R. Vishwanathan, T.A. Wilson, R.J. Nicolosi, Bioavailability of a nanoemulsion of lutein is greater than a lutein supplement, *Nano Biomed. Eng*. 1, 38–49 (2009)

[7] M.M.M. Affandi, T. Julianto, A.B.A. Majeed, Enhanced oral bioavailability of astaxanthin with droplet size reduction, *Food Sci. Technol. Res*. 18, 549–554 (2012)

[8] F. Miguel, A. Martin, T. Gamse, M.J. Cocero, Supercritical anti solvent precipitation of lycopene: Effect of the operating parameters, *J. Supercrit. Fluids* 36, 225–235 (2006)

[9] P. Boonnoun, H. Nerome, S. Machmudah, M. Goto, A. Shotipruk, Supercritical anti-solvent micronization of chromatography purified marigold lutein using hexane and ethyl acetate solvent mixture, *J. Supercrit. Fluids* 80, 15–22 (2013)

[10] H. Nerome, S. Machmudah, R. Fukuzato, T. Higashiura, Y.S. Youn,Y.W. Lee, M. Goto, Nanoparticle formation of lycopene/ß-cyclodextrin inclusion complex using supercritical antisolvent precipitation, *J. Supercrit. Fluids* 83, 97–103 (2013)

[11] H. Nerome, S. Machmudah, Wahyudiono, R. Fukuzato, T. Higashiura, H. Kanda, M. Goto, Effect of solvent on nanoparticle production of ß-Carotene by a supercritical antisolvent process, *Chem. Eng. Technol*. 39, 1771–1777 (2016)

[12] S. Li, Y. Zhao, Preparation of zein nanoparticles by using solution-enhanced dispersion with supercritical CO_2 and elucidation with computational fluid dynamics, *Int. J. Nanomed*. 12, 3485–3494 (2017)

[13] K. Murakami, M. Honda, R. Takemura, T. Fukaya, M. Kubota, Wahyudiono, H. Kanda, M. Goto, The thermal *Z*-isomerization-induced change in solubility and physical properties of (all-*E*)-lycopene, *Biochem. Biophys. Res. Commun*. 491, 317–322 (2017)

[14] J.L. Cooperstone, R.A. Ralston, K.M. Riedl, T.C. Haufe, R.M. Schweiggert, S.A. King, C.D. Timmers, D.M. Francis, G.B. Lesinski, S.K. Clinton, S.J. Schwartz, Enhanced bioavailability of lycopene when consumed as *cis*-isomers from tangerine compared to red tomato juice, a randomized, cross-over clinical trial, *Mol. Nutr. Food Res*. 59, 658–669 (2015)

[15] J. Hempel, C.N. Schädle, S. Leptihn, R. Carle, R.M. Schweiggert, Structure related aggregation behavior of carotenoids and carotenoid esters, *J. Photochem. Photobiol. A Chem*. 317, 161–174 (2016)

[16] M. Honda, K. Murakami, Y. Watanabe, T. Higashiura, T. Fukaya, Wahyudiono, H. Kanda, M. Goto, The *E*/*Z* isomer ratio of lycopene in foods and effect of heating with edible oils and fats on isomerization of (all-*E*)-lycopene, *Eur. J. Lipid Sci. Technol*. 119, 1600389 (1–9) (2017)

[17] M. Honda, N. Takahashi, T. Kuwa, M. Takehara, Y. Inoue, T. Kumagai, Spectral characterisation of *Z*-isomers of lycopene formed during heat treatment and solvent effects on the *E*/*Z* isomerisation process, *Food Chem*. 171, 323–329 (2015)

[18] M. Honda, T. Kudo, T. Kuwa, T. Higashiura, T. Fukaya, Y. Inoue, C. Kitamura, M. Takehara, Isolation and spectral characterization of thermally generated multi-*Z*-isomers of lycopene and the theoretically preferred pathway to di-*Z*-isomers, *Biosci. Biotechnol. Biochem*. 81, 365−371 (2017)

[19] U. Hengartner, K. Bernhard, K. Meyer, G. Englert, E. Glinz,Synthesis, isolation, and NMR-spectroscopic characterization of fourteen (*Z*)-isomers of lycopene and of some acetylenic didehydro- and tetradehydrolycopenes, *Helv. Chim. Acta* 75, 1848–1865 (1992)

[20] K. Fröhlich, J. Conrad, A. Schmid, D.E. Breithaupt, V. Bohm, Isolation and structural elucidation of different geometrical isomers of lycopene, *Int. J. Vitam. Nutr. Res*. 77, 369–375 (2007)

[21] J. Milanowska, A. Polit, Z. Wasylewski, W.I. Gruszecki, Interaction of isomeric forms of xanthophyll pigment zeaxanthin with dipalmitoylphosphatidylcholine studied in monomolecular layers, *J. Photochem. Photobiol. B*: Bio. 72, 1–9 (2003)

[22] W. Christoph, J. Michael, Thermal isomerization of lycopene, WO2002072509 A, (2002)

[23] M. Takehara, T. Kuwa, Y. Inoue, C. Kitamura, M. Honda, Isolation and characterization of (15*Z*)-lycopene thermally generated from a natural source, *Biochem. Biophys. Res. Commun*. 467, 58–62 (2015)

[24] M. Honda, Y. Watanabe, K. Murakami, R. Takemura, T. Fukaya, Wahyudiono, H. Kanda, M. Goto, Thermal isomerization pre-treatment to improve lycopene extraction from tomato pulp, *LWT-Food Sci. Technol*. 86, 69–75 (2017)

[25] I. Gamlieli-Bonshtein, E. Korin, S. Cohen, Selective separation of *cis-trans* geometrical isomers of ß-carotene via CO_2 supercritical fluid extraction, *Biotechnol. Bioeng*. 80, 169–174 (2002)

[26] A. Estrella, J.F. López-Ortiz, W. Cabri, C. Rodrı×guez-Otero, N. Fraile, A.J. Erbez, J.L. Espartero, I. Carmona-Cuenca, E. Chaves, A. Muñoz-Ruiz, Natural lycopene from *Blakeslea trispora*: all-*trans* lycopene thermochemical and structural properties, *Thermochim. Acta* 417, 157–161 (2004)

[27] H. Miyauchi, H. Kitagaki, T. Nakamura, S. Nakanishi, J. Kawai, Analysis of compound ratios of titanium dioxides with various crystallite sizes using X-ray diffraction broadenings, *Adv. X-Ray Chem. Anal. Jpn.* 41, 75–84 (2010)

Chapter 4

Crystallization of acetaminophen using swirl mixing micro device

4-1. Introduction

The fabrication of acetaminophen particles via supercritical antisolvent process with CO_2 as an antisolvent was studied. The experiments were conducted at temperatures of 35 – 50 °C and pressures of 8 – 15 MPa with 5 – 15 ml/min CO_2 flow rates. As a starting material, acetaminophen powder was dissolved in dimethylformamide (DMF). Results of UV–vis spectrophotometry and GC–MS (gas chromatography mass spectrometry) analysis showed that there was no remaining DMF solvent in the acetaminophen particles products. It indicated that CO_2 has successfully removed DMF from acetaminophen particles products. The surface characterization by using fourier transform infrared spectroscopy (FT–IR) showed that the CO_2 solvent did not impregnate to the acetaminophen particles products. Results from scanning electron microscope (SEM) images showed that the acetaminophen particles products were successfully prepared in non–spherical shape morphologies with size less than 1 μm. Based on the result, this process seems a powerful method to modify the acetaminophen powder physically such as particle size reduction.

Nano– and microparticles have been known to have widespread applications in pharmaceutical field and catalysis reaction. They also have been used in coloring industry to produce and improve the duration and the brightness of inks, toners and paints, and in the electric field to produce of the high–temperature superconductors [1]. Based on this application purpose, several techniques have applied to produce these particles, such as spray–

drying, freeze–drying, liquid antisolvent crystallization, and ball milling processes. These techniques have several drawbacks, such as the coarse particles generation with broad particle size distribution, degradation of the product may occur due to mechanical or thermal stresses, or contamination of particles with organic solvents or other toxic substances [2]. In the spray drying process, the feed solution containing the solute is atomized via a nozzle into droplets. Due to the high surface area of these droplets and the contact with the drying gas during process, these droplets may dry rapidly. The rapid solvent removal to generate particle products may avoid the dried powder products from overheating or degrading products. However, Sosnik and Seremeta [3] reported that drug degradation is not anticipated and may occur during spray drying process. The wide size distribution of particles products and the high residual solvent in the final products when the liquid antisolvent crystallization technique was used [4]. The long–time process was also needed in this process. Therefore, different alternative techniques are being investigated. In addition, the morphology of particles may give a significant impact on the dissolution rate and can also have an intriguing effect on particle functions [5,6]. Sen Gupta [6] reported that the particles morphology are important factors which influences on the particle behavior in blood flow in terms of cell–particle interactions, convective, and diffusive transport, lateral margination, target site, or cell binding and cellular internalization.

In the present work, supercritical carbon dioxide ($SCCO_2$) was employed as a media to produce particles from acetaminophen dissolved in dimethylformamide (DMF) in nano– and microscales. Generally, there are two main techniques to produce particles by using supercritical fluid: rapid expansion of supercritical solutions (RESS) and supercritical antisolvent (SAS) techniques. In RESS technique, supercritical fluid was employed as a solvent while it would be as an antisolvent in SAS technique [7]. A supercritical fluid including $SCCO_2$ can be defined as any fluid which is at

conditions above its critical point. It has liquid–like densities with gas–like transport properties and moderate solvent power, which can be tuned with shifts in pressure and temperature. Due to these transport properties, supercritical fluid has been employed in different fields for different applications, such as extractions, chromatography, or particle generation [8–11]. When the supercritical fluid was applied to particles formation, the organic solvent used as a solvent media can be removed completely from the particles products due to the high solubility of this solvent in supercritical fluid. In addition, the amount of organic solvent used also can be reduced. In this work, CO_2 was used as an antisolvent to produce particles from acetaminophen in DMF via swirl mixing micro device under supercritical conditions. One of the important parts in the SAS device is mixing of organic solvent and supercritical fluid [12–14]. There are many types of mixer such as Y–shaped, nozzle–type, central–collision–type, and swirl mixer that have been developed in order to reduce the formation of large particle products and wide size distribution during particle production. Kawasaki et al. [13] informed that swirl mixer is one of effective mixer to fabricate small sized particles with a narrow size distribution. They applied micro swirl mixer for fabricating fine metal oxide particle by continuous supercritical water. The result showed that employing micro swirl mixer with diameter of 0.5 mm generated the average particle size of 20 nm.

Acetaminophen (also recognized as paracetamol, 4–acetaminophenol, 4–hydroxy acetanilide) is one of the most widely used medications in the world. It has been used as an antipyretic, non–opioid analgesic, and non–steroidal anti–inflammatory drug (NSAID) [15]. The chemical structure of this compound comprises of an aromatic ring substituted in para orientation by two groups: an acetamide and a hydroxyl. Due to the multiple conjugation

on this compound involving the benzene ring, the hydroxyl oxygen, the amide nitrogen, and the carbonyl carbon and oxygen, acetaminophen may have a high reactivity [16]. The benzene ring is highly reactive to electrophilic aromatic substitution in oxygen, nitrogen, and the hydroxyl acidic bonds. It has high solubility in DMF; the solubility is >1000 g of acetaminophen/kg of solvent [17]. DMF is completely miscible in water and is both chemically and thermodynamically stable. This solvent was also called as the universal solvent since it can dissolve a wide variety of organic and inorganic materials. It also was applied primarily in the pharmaceutical processing [18,19]. Several research groups have been conducted recrystallization of acetaminophen using CO_2 as an antisolvent under supercritical conditions [20–22]. Fusaro et al. [21] performed precipitation experiments of acetaminophen from solution in acetone using compressed CO_2 as an antisolvent. The recrystallization process was conducted in a batch system. They informed that the different operating conditions promote to different morphologies in a certain way and the specific antisolvent addition rate might be used to control the final particle size as well as the particle morphology. Rossmann et al. [22] also performed the $SCCO_2$ antisolvent to crystallize acetaminophen particles at pressures of 10 – 16 MPa and temperature of 40 ^{o}C. Several organic solvents such as ethanol, acetone and mixtures of ethanol and acetone were used as solvents. The acetaminophen particles morphologies are different when the varying solvent composition was applied, however the average size of the acetaminophen particles products is not much influenced. They concluded that the different strategies can be applied to tune

the properties of acetaminophen particles products through the $SCCO_2$ antisolvent process.

4-2. Materials and Methods

4-2-1. Materials

Acetaminophen ($C_8H_9NO_2$; 97.0%), dimethylformamide (C_3H_7NO; 99.5%), ethanol (C_2H_5OH; 99.5%) were obtained from Wako Pure Chemicals Industries Ltd., Japan. They were used without further purification. Carbon dioxide (CO_2: 99%) was supplied by Sogo Kariya Sanso, Inc. Japan. For preparing the acetaminophen solution, acetaminophen powder was dissolved in DMF to achieve concentrations of 7.5 mg/ml of solvent. This concentration was selected based on the previous researcher's report [20].

4-2-2. Supercritical CO_2 Antisolvent

Fig. 4-1 described the crystallization apparatus scheme using swirl mixing micro device under pressurized carbon dioxide. The main apparatus was high pressures pump for CO_2 and acetaminophen solution (PU–2086, Jasco, Japan; LC–6AD, Shimadzu, Japan), a heating chamber (WFO–400; EYELA, Tokyo, Japan), a swirl mixing device (4–1/16YSM–0.8–0.5–S, Sugiyama Shoji Co., Ltd., Japan) and back pressure regulator (BPR; AKICO,

Tokyo, Japan). The coil preheater made of 1/8 inch stainless–steel tubing (SUS316) with 300 cm length was placed in the heating chamber to introduce the CO_2 before entering to swirl mixing micro device. K–type thermocouples were inserted in the preheater and attached in the swirl mixing micro device to monitor the temperature during experiment. To monitor the particles generation pressures, the digital pressure gauge (NS NPG–500A, Nihon Seimitsu Kagaku co., ltd, Japan) was assembled on the 1/16 inch stainless–steel tubing (SUS316) and placed between particles products collector and BPR. In this work, the particle generation from acetaminophen solution with $SCCO_2$ antisolvent was carried out at temperatures of 35 – 50 ^oC and pressures of 8 – 15 MPa. The CO_2 and the acetaminophen solution flow rates were 5 – 15 ml/min and 0.25 ml/min, respectively. The crystallization process can be explained briefly as follow. Initially, the power of heating chamber was switched on to heat the swirl mixing micro device including preheater to a desired temperature. Once the desired temperature was achieved, CO_2 was pumped into the crystallization apparatus system via the 1/16 inch stainless–steel capillary tube at a desired pressure. A BPR was employed to keep a constant pressure during crystallization process. Next, the acetaminophen solution was injected into the swirl mixing micro device upon the attainment of the desired conditions. The delivery of acetaminophen solution was finished after 60 min; the fresh CO_2 was still pumped at around 60 min to remove the residual DMF solvent in the particles products. This step was needed to avoid the redissolved of particles products in DMF solvent during depressurization process. After the process was completed, the CO_2 flow was stopped and the

crystallization apparatus system was slowly depressurized to atmospheric pressure. Then the particles products were collected in the bottles and stored in vacuum desiccator at room temperature. These processes were done until analysis.

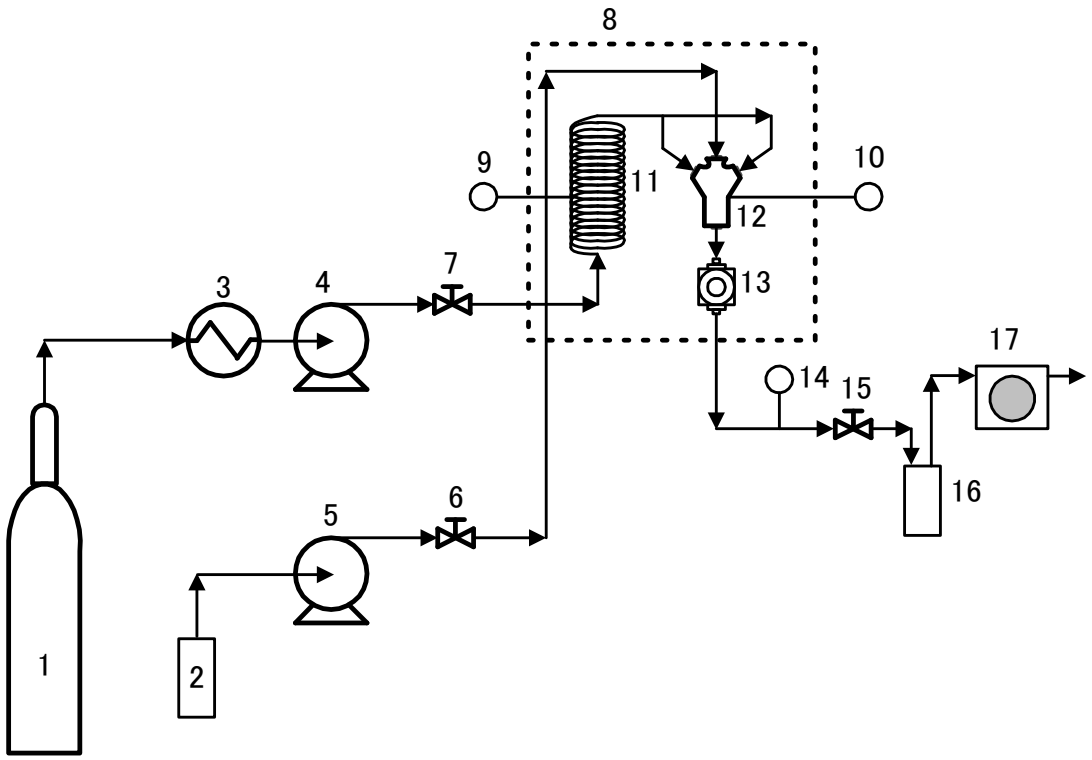

Fig. 4-1. Experimental apparatus: 1. CO_2 cylinder; 2. Feed solution; 3. Chiller; 4, 5. High pressure pump; 6, 7. Needle valve; 8. Oven; 9, 10. Temperature monitor; 11. SUS–316 pre–heater; 12. Swirl mixer; 13. Particles collector; 14. Pressure monitor; 15. BPR; 16. Solvent trap; 17. Wet flow meter.

4-2-3. Analytical methods

To identify the remaining DMF solvent in product, the acetaminophen particles products were dissolved in ethanol and analyzed by UV–vis spectrophotometry (V–550, Jasco Corporation, Japan). This analysis is simple to use and most analytes can be detected. The solution of acetaminophen particles products was placed and analyzed in a quartz cuvette with a 1 cm path length. By using a PC–driven scanning spectrophotometer operating in the fast scan mode, the allowing spectra of between 190 and 800 nm with 10 nm min^{-1} of bands were monitored and recorded. The acetaminophen particles products was also analyzed by using GC–MS (gas chromatography mass spectrometry) Hewlett Packard model 6890 series GC system and 5973 mass selective detector with a DB–5 MS capillary column (J&W Scientific, length 30 m, i.d. 0.25 mm, film 0.25 μm). The GC–MS carrier gas was He at a flow rate of 2 ml/min. 1 μl a solution in ethanol was injected. The injector temperature was 250 °C and the chromatographic exit to mass spectrometer interface temperature was 300 °C. The GC oven temperature was held at 45 °C for 1 min then programmed to increase at 5 °C/min to 300 °C. Electron ionization and positive ion mode were used. The NIST (National Institute of Standards and Technology) library of mass spectroscopy was used to identify the compounds. In order to understand the structure of acetaminophen after treatment by $SCCO_2$ antisolvent, the acetaminophen particles products collected at each operating condition were analyzed using a Spectrum Two FT–IR spectrophotometer (PerkinElmer Ltd., England). The spectra were

measured in attenuated total reflectance (ATR) mode (golden single reflection ATR system, P/N 10500 series, Specac) at 4/cm resolution. The scanning wave number ranged from 4000 to 400/cm. The morphology of the acetaminophen particles products was observed using a scanning electron microscope (SEM; S–4300, Hitachi, Japan) after gold coating. The diameters of them were measured from the SEM images using image analyzer software (Image J 1.42).

4-3. Results and Discussion

4-3-1. Product identification

In supercritical antisolvent, including CO_2 as a solvent, mass transfer is to be a key factor and it occurs between a droplet of organic solvent from feed solution and a compressed antisolvent to generate particles. This process was affected by the densities differences between solvent and antisolvent, viscosity, diffusivity, droplet or particle diameter, and solvent flow rate [23]. When $SCCO_2$ antisolvent was applied in pharmaceutical field application, it is able to produce various drugs formulation in nano–micro scale. **Fig. 4-2** shows the acetaminophen particles obtained (A) before and (B) after $SCCO_2$ antisolvent treatment. It was clearly observed that the original acetaminophen particles seem to have needle shape morphologies with size between 10 – 87 μm. Even, Biazar et al. [24] reported that acetaminophen particle size has been shown to follow a normal distribution with a mean particle size of 100 μm. While the particles size of acetaminophen after $SCCO_2$ antisolvent treatment was less than 1 μm with non–spherical shape morphologies. It indicates that the size of acetaminophen particle can be

reduced by using CO_2 as an antisolvent under supercritical conditions.

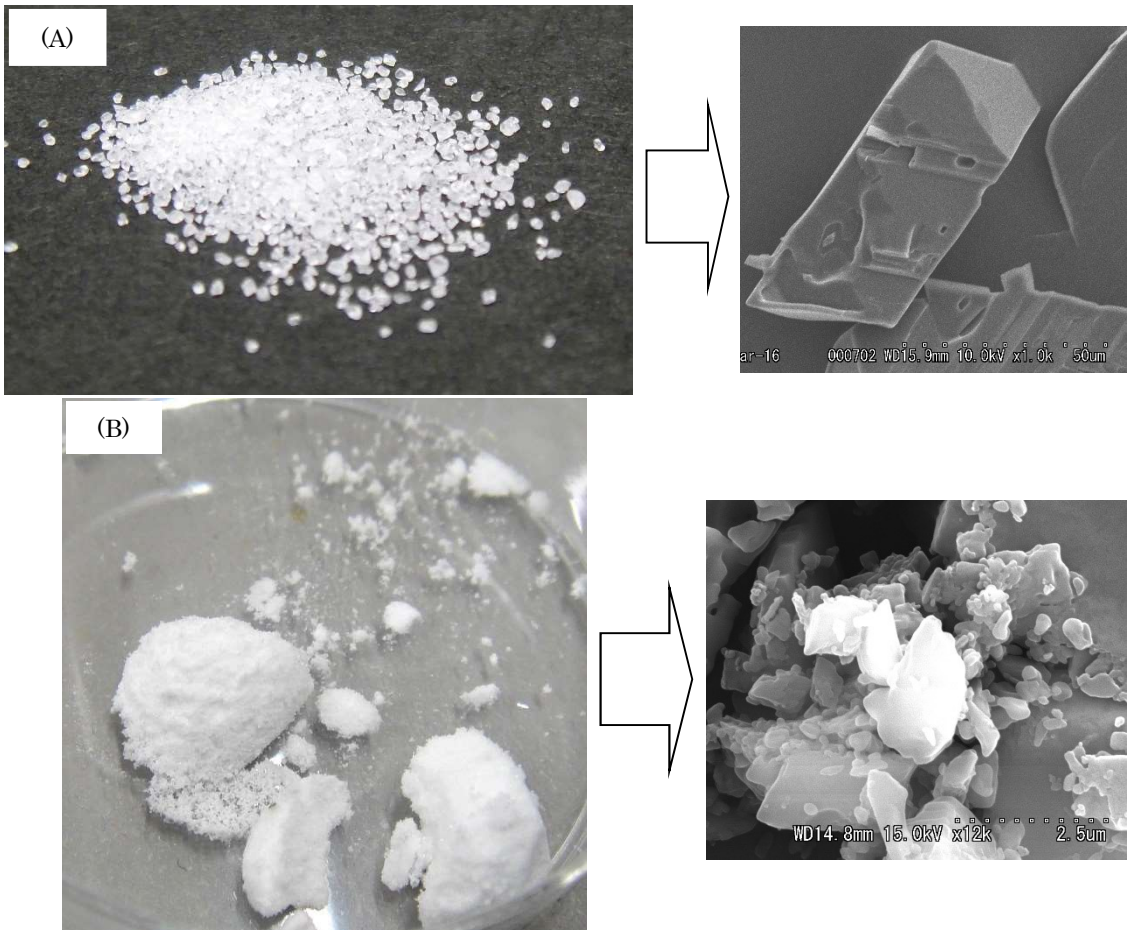

Fig. 4-2. Acetaminophen particles before (A) and after (B) treatment by $SCCO_2$ antisolvent at pressure of 10 MPa and temperature of 40 °C with CO_2 flow rate 10 ml/min.

Fig. 4-3 shows the UV–vis spectra of acetaminophen particles before and after $SCCO_2$ antisolvent treatment. Generally, the UV–vis spectrophotometry was applied to monitor chemical reaction, dissolution testing, and color determinations. This analysis is a non–destructive analytical technique and also an easy in sample preparation. Therefore, this tool was also the most

frequently used technique in pharmaceutical analysis [25,26]. Since this analysis is typically conducted on liquid solutions or suspensions, the acetaminophen particles before and after $SCCO_2$ antisolvent treatment were dissolved in ethanol with various concentrations. The UV–vis spectrophotometry for pharmaceutical applications concern light in the wavelength range 190 – 800 nm, qualitatively, acetaminophen in ethanol will be identified at 249 – 250 ± 0.5 nm [25]. As described in **Fig. 4-3**, the peak intensity at around 250 nm correspond to the acetaminophen compound in the ethanol solution was clearly detected. Conversely, the peak intensity at around 270 nm relation to the existence of DMF compound was not detected. There was no remaining DMF solvent in the acetaminophen particles products. It indicated that the DMF solvent in the acetaminophen particles products which retained in the particles products collector by placing stainless filter was successfully removed with the flowing CO_2 under supercritical fluid conditions [27]. Similar results were also obtained when the acetaminophen particles before and after $SCCO_2$ antisolvent treatment were analyzed by GC–MS. The DMF compound which used as a solvent was not detected. **Fig. 4-4** shows the GC–MS spectra of them. The GC–MS is well–known as a powerful tool to identify aromatic and aliphatic compounds. Prior to analysis using GC–MS, about 1 mg of the acetaminophen particles before and after treatment by $SCCO_2$ antisolvent were also diluted with 2 ml ethanol at room temperature. Then, these solutions were injected in the GC–MS apparatus immediately. The identities of those compounds determined through a match of mass spectra in the GC–MS computer library are reliable.

As shown in **Fig. 4-4A**, cyanoacetophenone (1), acetaminophen (2), and metacetamol (3) were detected clearly on the GC–MS chromatogram with retention time 3.78, 27.76, and 30.83 min, respectively. These compounds were also found in the GC–MS spectra of acetaminophen particles products after treatment by $SCCO_2$ antisolvent with the same retention time (see **Fig. 4-4B, 4-4C** and **4-4D**). There was no peak correspond to the existence of DMF compound. These results suggested that the DMF solvent in the collected acetaminophen particles products has been removed with the flowing CO_2 under these conditions. Kim et al. [27] conducted experiment for nanoparticle production from atorvastatin calcium by the $SCCO_2$ antisolvent. They reported that the various organic solvents including DMF that used as a solution solvent could be removed completely by the flowing CO_2 at temperature of 40 ^{o}C and pressure of 12 MPa.

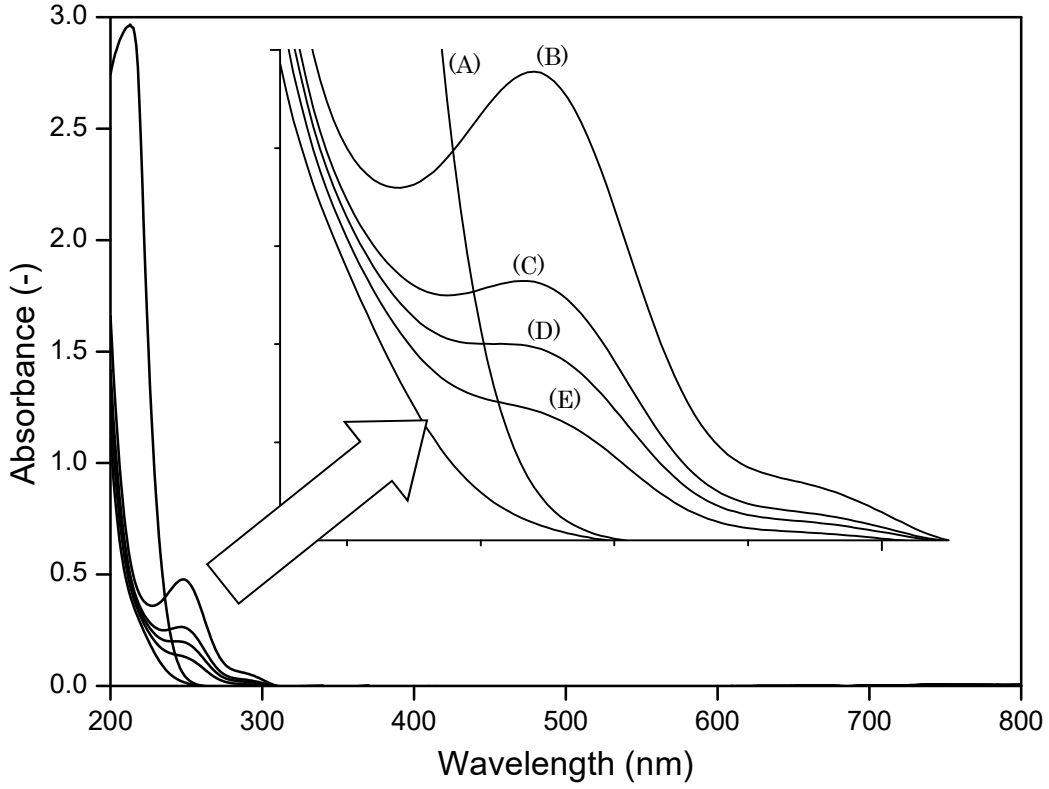

Fig. 4-3. UV–vis spectra of acetaminophen particles products at temperature of 40 °C and pressure of 10 MPa with various CO_2 flow rates: (A) DMF in ethanol, (B) Acetaminophen, (C) 15 ml/min, (D) 10 ml/min and (E) 5 ml/min.

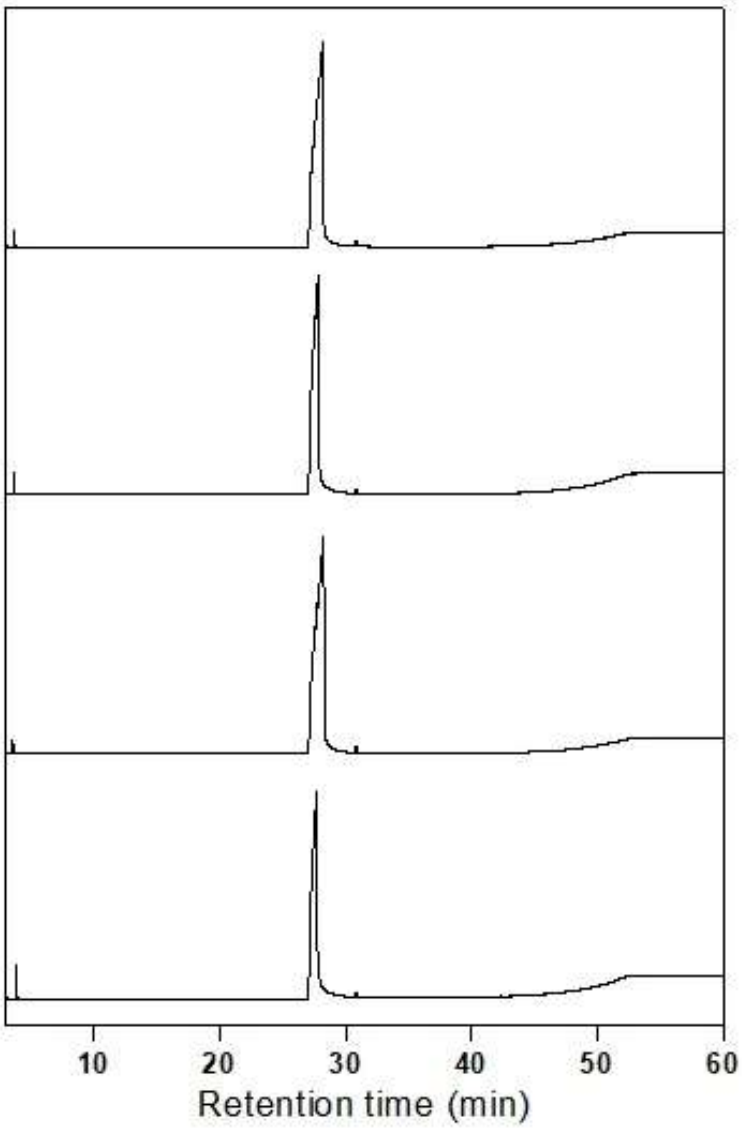

Fig. 4-4. GC–MS chromatogram of acetaminophen particles before (A) and after treatment by $SCCO_2$ antisolvent at pressure of 10 MPa and temperature of 40 °C with CO_2 flow rates (B) 5, (C) 10, and (D) 15 ml/min, respectively.

4-3-2. Product characterization

In order to investigate the possibility of structural change of acetaminophen molecules after $SCCO_2$ antisolvent treatment, the acetaminophen particles products were characterized by FT–IR spectroscopy, in the wave numbers region of 4000 – 400/cm. Infrared spectroscopy is an analytical technique that allows to identify the unknown substances and the types of chemical bonds of the compounds in those substances content. Acetaminophen powder (without any treatment) was used directly as a control. FT–IR spectra of acetaminophen particles before and after $SCCO_2$ antisolvent treatment are shown in **Fig. 4-5**. Every molecule is consisted of many different chemical bonds, and these bonds are slightly elastic and can stretch, bend, or vibrate. **Table 4-1** summarized the main regions of an infrared spectrum for single, double, or triple or bonds to hydrogen and others [28]. Every distinctive functional group on the chemical compound will absorb radiation in certain frequencies, such as the OH groups absorb strongly at 3,200 – 3,600/cm, the CO groups absorb strongly at 1,710/cm; and the CH_3 groups absorb strongly at 1,450 and 1,375/cm [28,29]. Therefore, some differences exist at each FT–IR spectra due to their structure properties. However, the fingerprint regions which can be applied to identify a chemical compound due to its uniqueness are 1,450 to 600/cm [29]. At these regions, there was no diversity on the FT–IR spectra of acetaminophen particles before and after $SCCO_2$ antisolvent treatment. It indicated that the acetaminophen particles products obtained by $SCCO_2$ antisolvent treatment

are within a similar functional group as acetaminophen particles before CO_2 treatment. It clearly indicated that CO_2 did not impregnate to the acetaminophen particles products or there was no remaining DMF solvent in the acetaminophen particles products. At these conditions, DMF solvent able to dissolve the acetaminophen compound and at the same time be miscible with CO_2 when the low solubility of acetaminophen in CO_2 was very low [20,30,31]. As a result, DMF solvent can be removed completely by CO_2 leaving the acetaminophen particles as products. These results are in good agreement with the results obtained by UV–vis spectrophotometry and GC–MS which not shows the peak intensity at around 270 nm and the peak chromatogram correspond to the existence of DMF compound.

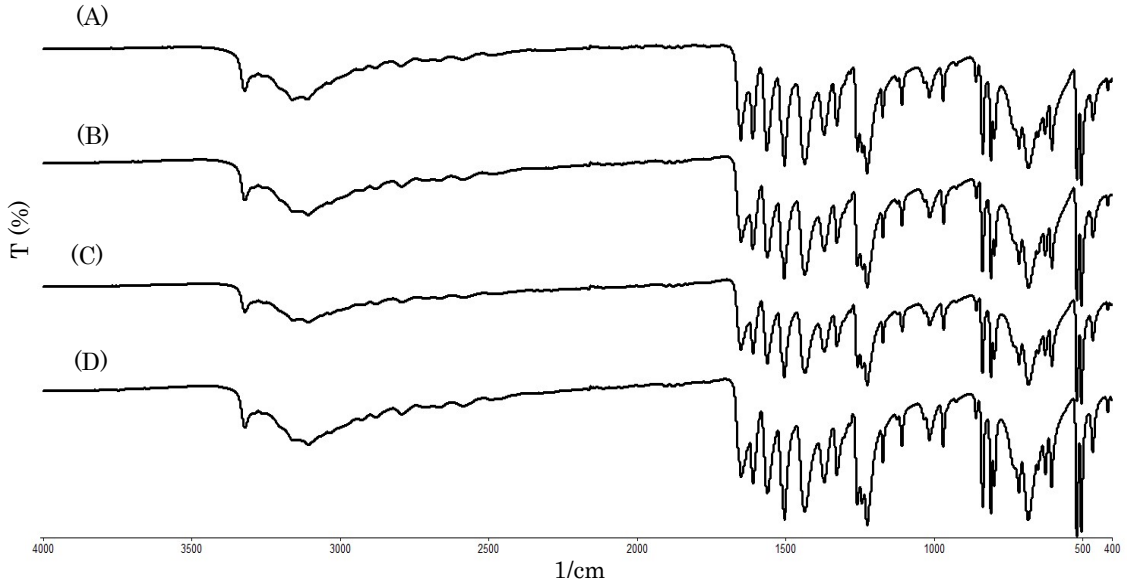

Fig. 4-5. FT–IR spectrum of acetaminophen particles before (A) and after treatment by $SCCO_2$ antisolvent at pressure of 10 MPa and temperature of 40 °C with CO_2 flow rates (B) 5, (C) 10, and (D) 15 ml/min, respectively.

Table 4-1 Wave number assignments of FT–IR spectra

Wave number [1/cm]	Functional groups
3500 – 600	O–H bonds
2800–3000	C–H Lipid region
1504	In–plane CH bending vibration from the phenyl rings
1482	Benzene
1456	CH_3 bending vibration (lipids and proteins)
1312–1317	Amide III band components of proteins collagen
1255	Amide III
1244/5	PO–2 asymmetric (phosphate I)
1206	Amide III Collagen
1180–300	Amide III band region
1145	Phosphate & oligosaccharides
1105	Carbohydrates
1030	Collagen
1020–50	Glycogen
1000–350	Region of the phosphate vibration carbohydrate residues attached to collagen and amide III vibration (in collagen)
1000–200	C–OH bonds in oligosaccharides such as mannose & galactose
1000–140	Protein amide I absorption
940	Carotenoid
892	C–C, C–O deoxyribose
600–900	CH out–of–plane bending vibrations
472 – 521	torsion and ring torsion of phenyl

4-3-3. Effect of CO_2 flow rate

Fig. 4-6 shows SEM images of acetaminophen particles before and after treatment by $SCCO_2$ antisolvent at various CO_2 flow rates. Apparently, the morphology of acetaminophen particles products was almost similar and agglomeration was found during formation of acetaminophen particles at each condition. It indicated that the formation of acetaminophen particles from acetaminophen solution by using $SCCO_2$ antisolvent at various CO_2 flow rates is essentially the same process. The process consisted of mixing of solution and antisolvent, generation of supersaturation, nucleation, and growth by coagulation and condensation, followed by agglomeration [4]. Generally, the increasing flow rate in supercritical antisolvent processes may result several effects. An increase in CO_2 flow rate at a constant feed solution flow rate will decrease the size of particle products. This phenomenon was probably due to the increase in the Reynolds number affected by the CO_2 flow rate, thus turbulence increased which resulted in a better mixing between the solvents turbulence, and thus may promote to the precipitation process [32].

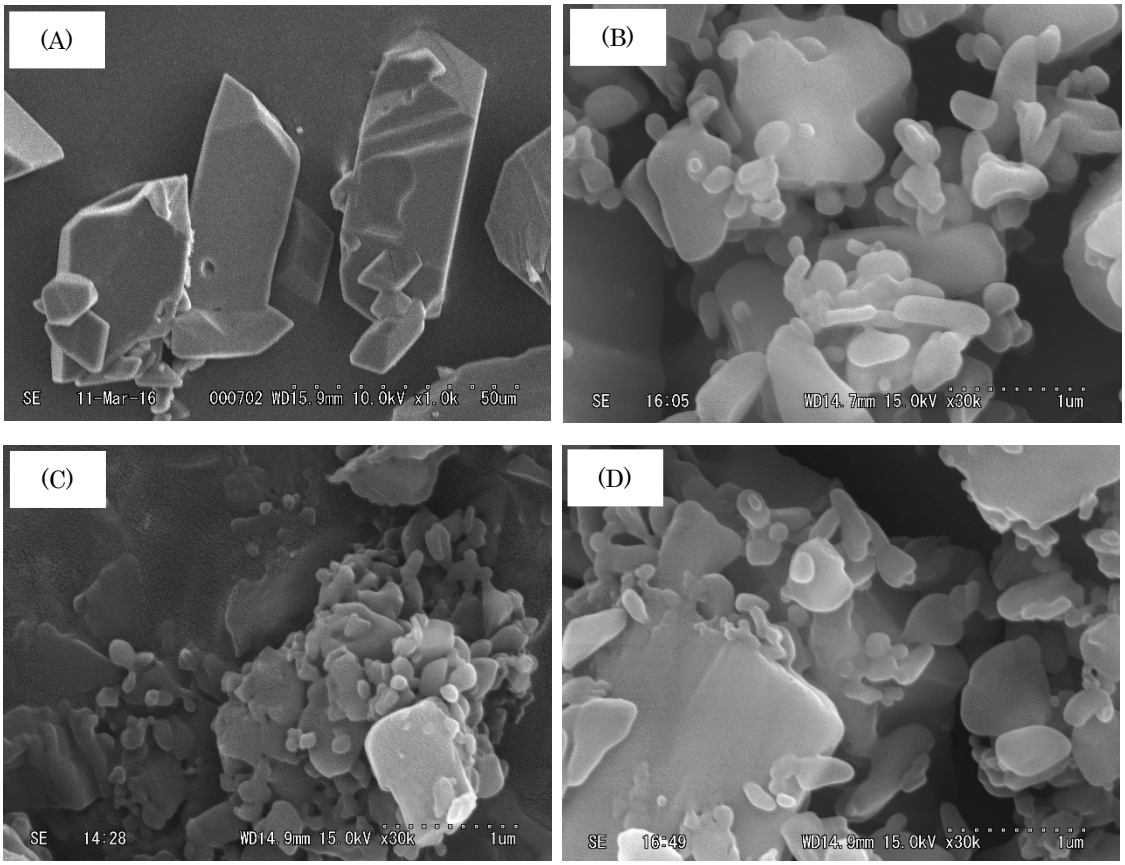

Fig. 4-6. SEM images of (A) acetaminophen particles before and after treatment by $SCCO_2$ antisolvent at pressure of 10 MPa and temperature of 40 °C with CO_2 flow rate (B) 5, (C) 10, and (D) 15 ml/min, respectively.

In this work, using the Image J 1.42 tool, from each image which shown in **Fig. 4-6**, at least 250 different acetaminophen particles products were randomly selected, and their size were measured to generate the particle size distribution. Due to the limitation of the analytical equipment, the dynamic light scattering (DLS) analysis was not performed to characterize the acetaminophen particles products. As shown in **Fig. 4-7**, although the change of CO_2 flow rate did not seem to give a high effect on the size of acetaminophen particles products, it can be seen that the higher CO_2 flow rate resulted in the narrow particle size distribution. At 5 ml/min CO_2 flow rate, the acetaminophen particles products were generated with size ranges of 70 – 620 nm. It seems that the acetaminophen particles in 170 – 370 nm diameters were formed dominantly. Conversely, the narrower particle size distribution was obtained when the $SCCO_2$ antisolvent was conducted at the same condition with 15 ml/min CO_2 flow rate. The acetaminophen particles size ranges were 70 – 570 nm and the size of particles in 170 – 320 nm diameters were produced dominantly. It seemed that the higher CO_2 flow rates might promote the mass transfer rates between CO_2 with organic solvent out of the droplets and enhanced the system turbulence, thus increased the supersaturation ratio and resulted in small particles. At higher CO_2 flow rate, the composition of the bulk fluid is decreased by CO_2 flow rate which affects CO_2 dissolving in DMF as a solvent solution. As a result, the solubility of the acetaminophen in DMF will be reduced and smaller particles might be produced [12,33,34]. Imsanguan et al. [33] reported that the mean particle size decreased with increasing CO_2 flow rate in all experiments when they

performed $SCCO_2$ antisolvent to precipitate andrographolide from *Andrographis paniculata* extracts. They explained that when CO_2 flow rate is rised, the kinetic energy of mass transfer between CO_2 with solution droplet is also increased leading high mass transfer resulting in small droplets, high supersaturation, small particles. Guha et al. [34] also informed that at higher CO_2 flow rates, higher supersaturation levels for shorter period promote to formation of more particles with a narrower size distribution. Conversely, the fluid phase produced in the $SCCO_2$ antisolvent system loaded larger quantities of the DMF solvent when the CO_2 flow rate decreases. Next, the solubilization and solute precipitation processes may occur slowly to yield the acetaminophen larger particles with broader particle size distribution. In detail, Imsanguan et al. [33] explained that the change in CO_2 flow rate not only influences kinetic energy of $SCCO_2$, but also the composition of fluid phase. When the ratio of $SCCO_2$ to organic solution is decreased by decreasing CO_2 flow rate, the fugacity coefficient also decreases promoting to higher solubility and a lower precipitation yield. Next, the particles formation process shifts toward the growth process and therefore larger particles would be produced. By the way, the result is, of course, good news in terms of reducing crystalline acetaminophen drug particles size. Because particles size is one of the critical parameters that determine the dissolution rate of the drug in the biological fluids. Bojnanska et al. [35] reported that particle size and particle size distribution have a significant effect on the bioavailability of those drugs that have poor solubility in water. They informed that the particle size distribution of the drug substance seems to be critical quality attributes

affecting the dissolution rate of the drug substance released from the final peroral drug formulation. Judging from the results, it could be said that the size of acetaminophen particles has been successfully reduced from microscale to nanoscale by using $SCCO_2$ antisolvent.

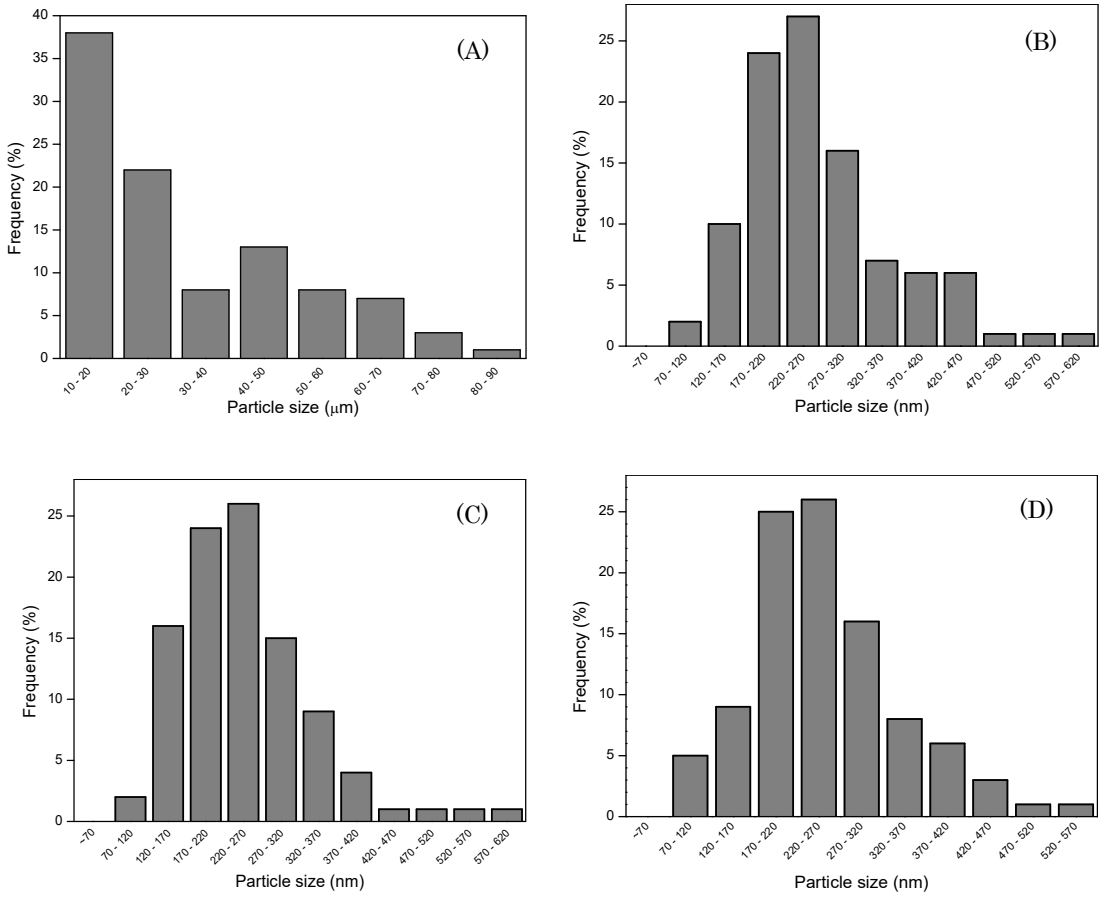

Fig. 4-7. The particle size distribution of (A) acetaminophen particles before and after treatment by $SCCO_2$ antisolvent at pressure of 10 MPa and temperature of 40 °C with CO_2 flow rate (B) 5, (C) 10, and (D) 15 ml/min, respectively.

4-3-4. Effects of pressure and temperature

It was well known that the advantages of using supercritical fluids, such as CO_2, rather than other solvents are mainly due to their physical and chemical properties being intermediate between those of liquids and gases. As informed above, under supercritical conditions, the liquid–like density enhances the solvating power of CO_2 compared to the gaseous state, and the gas–like mass transport properties enhances the diffusion rate compared to the liquid state. They can be tuned by changing temperature and/or pressure. Next, this rapid transport properties of CO_2 can be utilized as a media to produce particles in nano–micro scale. **Fig. 8** and **9** show the acetaminophen particles products and their size produced by using $SCCO_2$ antisolvent at various operating pressures and temperatures. Generally, the increasing operating pressure of $SCCO_2$ antisolvent will be followed by the smaller (shorter and thinner) particles products [33,36,37]. When the operating pressure is high, it is in favor of nucleation process to create and produce a lot of nucleus. Consequently, the particles products will be obtained with smaller size. As shown in **Fig. 4-8**, it seems that the similar size of acetaminophen particles products with non–spherical shape morphologies were found at each condition. Their morphologies seem to exhibit as plate–like or needle–like shapes. However, from **Fig. 4-9**, it could be seen that the particles size with ranges of 220 – 520 nm were obtained dominantly when the experiment was performed at pressure of 15 MPa and temperature of 35 ^{o}C with 10 ml/min CO_2 flow rate. In comparison, the particles size with ranges

of 220 – 620 nm were found prominently when the experiment was performed at the same condition with the lower pressure at around 8 and 10 MPa. The higher operating pressures resulted the higher CO_2 density, and it was well known that the density of supercritical fluid had high influence on the mass transfer between organic solvent and supercritical fluid during precipitation process. The higher CO_2 density leads to the stronger the dissolving abilities of $SCCO_2$ to DMF solvent. Next, the rapid mass transfer between CO_2 and DMF solvent causes high supersaturations for the acetaminophen and promotes in the precipitation of acetaminophen smaller particles products. Imsanguan et al. [33] reported that the changing the operating pressure is the main reason for changing the $SCCO_2$ density. At higher pressure, the density of CO_2 is higher to result in the difference in density between pure solvent and pure CO_2 decreases promoting to a small maximum droplet radius and short average lifetime of a droplet. These phenomenon leads to high mass transfer rate, high supersaturation, fast nucleation and crystal growth rate and small crystal particles. Li et al. [37] conducted experiments for recrystallization and size control of puerarin using the $SCCO_2$ antisolvent process. They reported that when operating pressure was high, it was in favor of nucleation, which created a lot of nucleus and thus we obtained crystals with smaller size. On the contrary, when the operating pressure was low, the solvent was not fully expanded, more solvent existed between particles, and the time of crystal growth was prolonged and larger particles were formed. Based on the results, although there is no significant effect of the increasing operating pressure in the particle size and particle size distribution of

acetaminophen particles products, it seems that the increasing operating pressure of $SCCO_2$ antisolvent may enhance the nucleation rate and particles growth of acetaminophen to form smaller sized particles [37].

Fig. 4-8 and **4-9** also show that the increasing operating temperature of $SCCO_2$ antisolvent treatment at the same operating pressure and CO_2 flow rate was followed by increasing the size of acetaminophen particles products. As shown in **Fig. 4-9**, the operating temperature of 35 °C with pressure of 10 MPa and CO_2 flow rate yielded the acetaminophen particles products with size ranges of 120 – 970 nm with an average particles size of 444 nm. While the acetaminophen particles products with size ranges of 70 – 620 nm and 120 – 920 nm with average particles sizes were 244 and 457 nm were obtained when the experiments were carried out at temperatures of 40 and 50 °C, respectively, with the same operating pressure and CO_2 flow rate. It seemed that the operating temperature may possess two different effects on the size of acetaminophen particles products [20,33,34]. It showed that the mean size of acetaminophen particles products at operating temperature of 35 °C was smaller than the mean size of acetaminophen particles products at operating temperature of 50 °C. At these conditions, the increasing operating temperature leads to the decreasing CO_2 density, as a result, the dissolving ability of CO_2 also decreases. Then supersaturation will decrease and the bigger size of acetaminophen particles products will be generated. Li et al. [20] informed that the solubility of acetaminophen in the DMF solvent may increase with increasing operating temperature when they performed

crystallization of acetaminophen micro–particle by using $SCCO_2$ antisolvent. As a result, the size of acetaminophen particles products will increase due to the supersaturation will be attained slower. Li et al. [37] confirmed that the bigger puerarin particles products were produced due to the supersaturation is decreased when the higher operating temperature was applied on the recrystallization puerarin under $SCCO_2$ conditions. Interestingly, the mean size of acetaminophen particles products at operating temperature of 40 ^oC was smaller than the mean size of acetaminophen particles products at operating temperature of 35 ^oC. It could be explained that the increasing operating temperature resulted the decreasing of the $SCCO_2$ density. Next, the diffusivity of the $SCCO_2$ may increase and the solute solubility in $SCCO_2$ will decrease so that the supersaturation will be achieved faster. Consequently, the acetaminophen particles products size will decrease. He et al. [38] investigated the effect of operating temperature on the $SCCO_2$ antisolvent to micronize natural carotene. The experiments were conducted at operating temperatures of 35 – 50 ^oC and operating pressures of 8 – 20 MPa. They reported that the increasing operating temperatures had no significant effect on the size of carotene particles products. Moreover, they obtained the carotene particles products with smaller size with increasing operating temperatures. In detail Imsanguan et al. [33] explained that there are two competition phenomena in the particle formation as the temperature changes under $SCCO_2$ conditions. First, a decline in $SCCO_2$ density leads to the $SCCO_2$ diffusivity to give resulting in high mass transfer rates and decreasing particle product size. Second, an increase in the solute solubility

will slow the supersaturation attainment and an increase in the particle product size. In addition, He et al. [38] also informed that the effect of operating temperature depends on the employed solvent, the type of solute, and other factors. Judging from the results, it could be said that the acetaminophen particle product size seemed increase with increasing operating temperature.

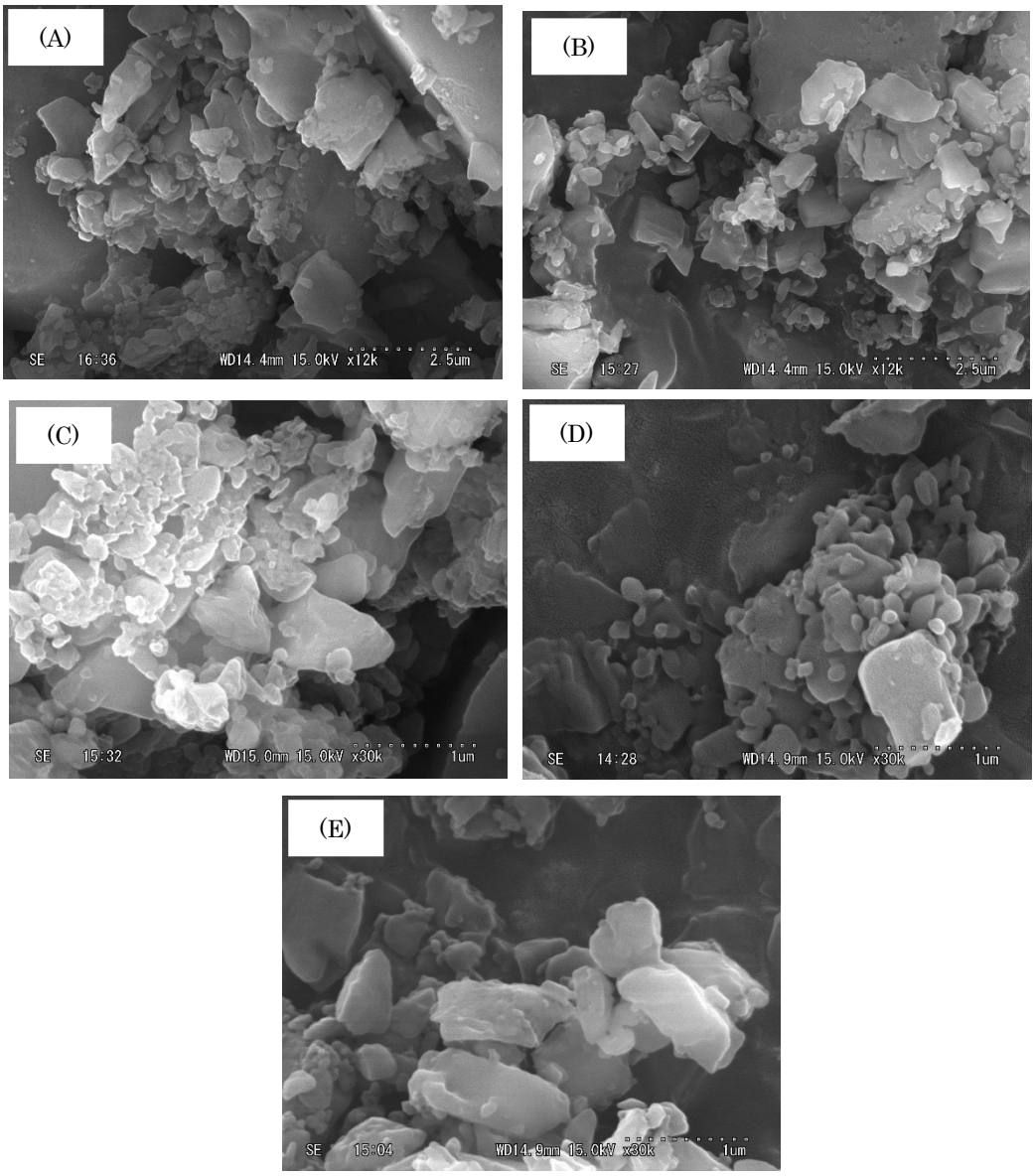

Fig. 4-8. SEM images of acetaminophen particles after treatment by $SCCO_2$ antisolvent at various operating conditions with CO_2 flow rate 10 ml/min: (A) 35 °C; 8 MPa, (B) 35 °C; 10 MPa, (C) 35 °C; 15 MPa, (D) 40 °C; 10 MPa and (E) 50 °C; 10 MPa.

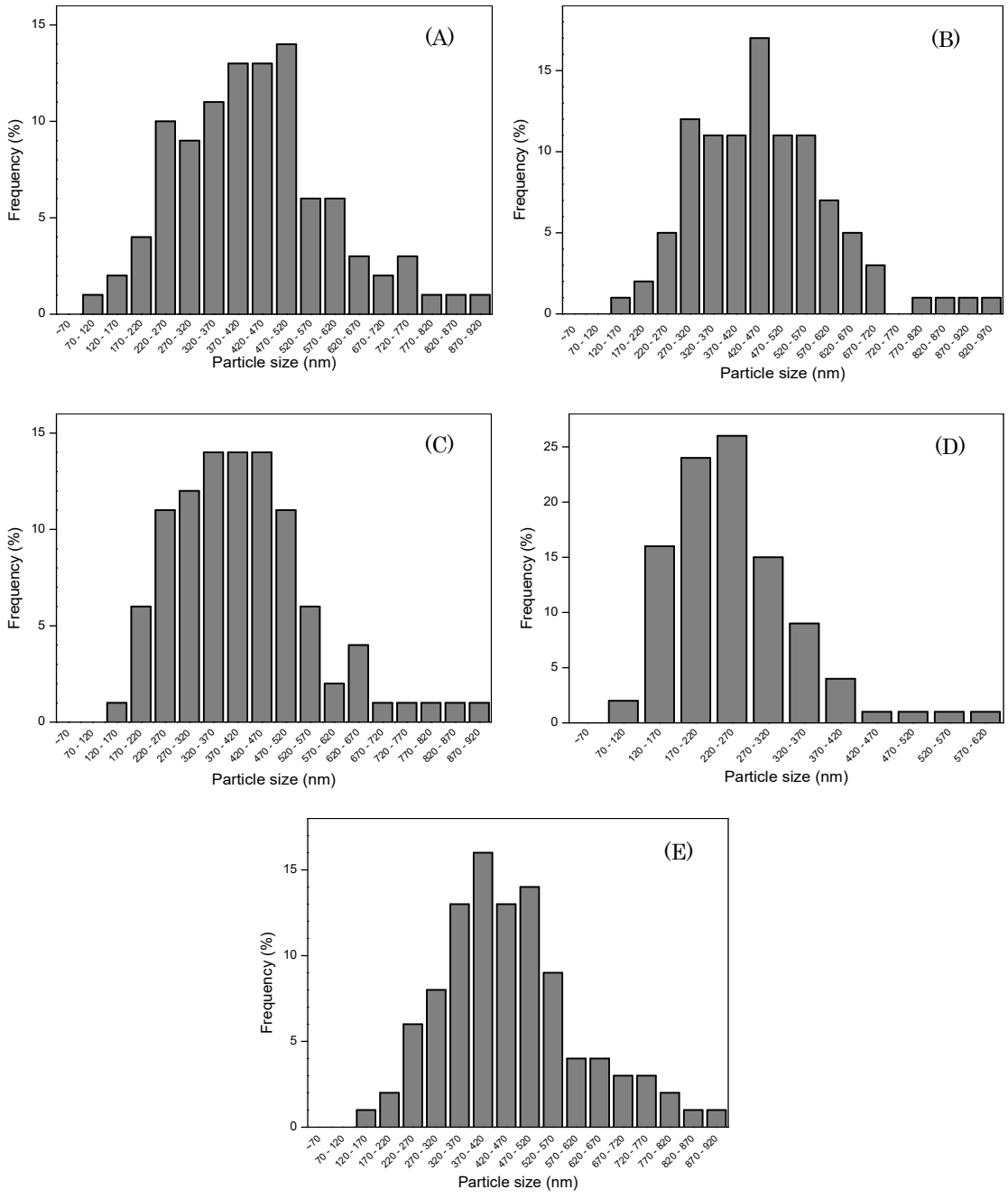

Fig. 4-9. The particle size distribution of acetaminophen particles after treatment by $SCCO_2$ antisolvent at various operating conditions with CO_2 flow rate 10 ml/min: (A) 35 °C; 8 MPa, (B) 35 °C; 10 MPa, (C) 35 °C; 15 MPa, (D) 40 °C; 10 MPa and (E) 50 °C; 10 MPa.

4-4. Conclusion

The production of acetaminophen particles via supercritical antisolvent process with CO_2 as an antisolvent has been demonstrated. The experiments were performed at temperatures of 35 – 50 ^{o}C and pressures of 8 – 15 MPa with 5 – 15 ml/min CO_2 flow rates. The acetaminophen powder which dissolved in DMF was used as a starting material. The spectra of UV–vis and GC–MS analysis showed that there was no remaining DMF solvent in the acetaminophen particles products. It indicated that CO_2 has successfully removed DMF from acetaminophen particles products. The surface characterization by using FTIR showed that the CO_2 solvent did not impregnate to the acetaminophen particles products. The SEM images showed that the acetaminophen particles products were successfully produced in non–spherical shape morphologies with size less than 1 μm. Finally, it could be said that this process seems a powerful method and to be an apt for size reduction of acetaminophen powder.

References

[1] Reverchon E, De Marco I, Adami R, et al. Expanded micro–particles by supercritical antisolvent precipitation: Interpretation of results. *J. Supercrit. Fluids*, 44:98–108 (200)

[2] Nunes AVM, Duarte CMM. Dense CO_2 as a Solute, Co–Solute or Co–Solvent in Particle Formation Processes: *A Review*. *Materials*, 4, 2017–2041 (2011)

[3] Sosnik A, Seremeta KP. Advantages and challenges of the spray–drying technology for the production of pure drug particles and drug-loaded polymeric carriers. *Adv. Colloid. Interface. Sci*, 223, 40–54 (2015)

[4] Thorat AA, Dalvi SV. Liquid antisolvent precipitation and stabilization of nanoparticles of poorly water soluble drugs in aqueous suspensions: Recent developments and future perspective. *Chem. Eng. J*, 181–182, 1–34 (2012)

[5] Truong NP, Whittaker MR, Mak CW, et al. The importance of nanoparticle shape in cancer drug delivery. *Expert Opin Drug Deliv*, 12, 129–142 (2015)

[6] Sen Gupta A. Role of particle size, shape, and stiffness in design of intravascular drug delivery systems: insights from computations, experiments, and nature. *Wiley Interdiscip Rev. Nanomed Nanobiotechnol*, 8:255–270 (2016)

[7] Reverchon E, Donsi G, Gorgoglione D. Salicylic Acid Solubilization in Supercritical CO_2 and Its Micronization by RESS. *J. Supercrit. Fluids*, 6, 241–248 (1993)

[8] Machmudah S, Zakaria, Sugeng W, et al. Lycopene extraction from tomato peel by–product containing tomato seed using supercritical carbon dioxide. *J Food Eng*,108, 290–296 (2012)

[9] Nerome H, Machmudah S, Wahyudiono, et al. Nanoparticle formation of lycopene/β–cyclodextrin inclusion complex using supercritical antisolvent precipitation. *J. Supercrit. Fluids,* 83:97–103 (2013)

[10] Goto M, Kanda H, Wahyudiono, et al. Extraction of carotenoids and lipids from algae by supercritical CO_2 and subcritical dimethyl ether. *J. Supercrit. Fluids*, 96, 245–251 (2015)

[11] Sanchez–Camargo ADP, Parada–Alfonso F, Ibanez E, et al. On–line coupling of supercritical fluid extraction and chromatographic techniques. *J. Sep. Sci*, 40,213–227 (2017)

[12] Baldyga J, Kubicki D, Shekunov BY, et al. Mixing effects on particle formation in supercritical fluids. *Chem. Eng. Res. Des,* 88,1131–1141 (2010)

[13] Kawasaki S. Sue K, Ookawara R, et al. Development of novel micro swirl mixer for producing fine metal oxide nanoparticles by continuous supercritical hydrothermal method. *J. Oleo. Sci,* 59, 557–562 (2010)

[14] Chhouk K., Wahyudiono, Kanda H, et al. Micronization of curcumin with biodegradable polymer by supercritical anti–solvent using micro swirl mixer. Front Chem Sci Eng inpress.
[15] Chiam E, Weinberg L, Bellomo R. Paracetamol: a review with specific focus on the haemodynamic effects of intravenous administration. Heart, *Lung and Vessels,* 7, 121–132 (2015)
[16] Waring RH, Steventon GB, Mitchell SC. Molecules of Death. 2rd ed. London WC2H 9HE: Imperial College Press, (2007)
[17] Granberg RA, Rasmuson AC. Solubility of paracetamol in pure solvents. *J. Chem. Eng. Data*, 44, 1391–1395 (1999)
[18] Pires LR, Guarino V, Oliveira MJ, et al. Ibuprofen-loaded poly (trimethylene carbonate–co–ε–caprolactone) electrospun fibres for nerve regeneration. *J Tissue Eng Regen Med,* 10, E154–E166 (2016)
[19] Gardella L, Colonna S, Fina A, et al. A Novel Electrostimulated Drug Delivery System Based on PLLA Composites Exploiting the Multiple Functions of Graphite Nanoplatelets. *ACS Appl Mater Interfaces*, 8, 24909–24917 (2016)
[20] Li G, Chu J, Song ES, et al. Crystallization of Acetaminophen Microparticle Using Supercritical Carbon Dioxide, *Korean. J. Chem. Eng*, 23, 482–487 (2006)
[21] Fusaro F, Mazzotti M, Muhrer G. Gas antisolvent recrystallization of paracetamol from acetone using compressed carbon dioxide as antisolvent. *Cryst. Growth. Des*, 4, 881–889 (2004)
[22] Rossmann M, Braeuer A, Leipertz A. Manipulating the size, the morphology and the polymorphism of acetaminophen using supercritical antisolvent (SAS) precipitation. *J.* Supercrit. Fluids. 82, 230–237 (2013)
[23] Chong GH, Spotar SY, Yunus R. Numerical Modeling of Mass Transfer for Solvent–Carbon Dioxide System at Supercritical (Miscible) Conditions. *J. Appl. Sci*, 9, 3055–3061 (2009)
[24] Biazar E, Beitollahi A, Rezayat SM, et al. Effect of the mechanical activation on size reduction of crystalline acetaminophen drug particles. *Int. J. Nanomedicine,* 4, 283–287 (2009)
[25] Miller R, Liggieri L. Bubble and Drop Interfaces. Leiden: Koninklijke Brill NV, (2011)
[26] Mullertz A, Perrie Y, Rades T. Analytical Techniques in the Pharmaceutical Sciences. New York: Springer Science+Business Media LLC, (2016)
[27] Kim MS, Song HS, Park HJ, et al. Effect of solvent type on the nanoparticle formation of atorvastatin calcium by the supercritical antisolvent process. *Chem Pharm Bull (Tokyo),* 60, 543–547 (2012)
[28] Movasaghi Z, Rehman S, ur Rehman DI. Fourier transform infrared (FTIR) spectroscopy of biological tissues. *Appl. Spectrosc. Rev,* 43, 134–179 (2008)

[29] Dash A, Somnath S, Tolman J. Pharmaceutics: Basic Principles and Application to Pharmacy Practice. *Academic Press. San Diego*: Elsevier Inc. (2014)
[30] Bristow S, Shekunov BY, York P. Solubility analysis of drug compounds in supercritical carbon dioxide using static and dynamic extraction systems. *Ind. Eng. Chem. Res,* 40, 1732–1739 (2001)
[31] Jodecke M, Kamps APS, Maurer G. An experimental investigation on the influence of NaCl on the solubility of CO_2 in (N,N–dimethylmethanamide + water). *Fluid Phase Equilib* 334, 106–116 (2012)
[32] Sui X, Wei W, Yang L, et al. Preparation, characterization and in vivo assessment of the bioavailability of glycyrrhizic acid microparticles by supercritical anti–solvent process. *Int. J.* Pharm, 423, 471–479 (2012)
[33] Imsanguan P, Pongamphai S, Douglas S, et al. Supercritical antisolvent precipitation of andrographolide from Andrographis paniculata extracts: effect of pressure, temperature and CO_2 flow rate. *Powder. Technol,* 200, 246–253 (2010)
[34] Guha R, Vinjamur M, Mukhopadhyay M. Demonstration of mechanisms for coprecipitation and encapsulation by supercritical antisolvent process. *Ind. Eng. Chem. Res*, 50, 1079–1088 (2010)
[35] Bojnanska E, Kalina M, Parizek L, et al. Determination of critical parameters of drug substance influencing dissolution: a case study. *BioMed Res Int*, (2014); (2014) doi: http://dx.doi.org/10.1155/2014/929248.
[36] Cardoso MAT, Monteiro GA, Cardoso JP, et al. Supercritical antisolvent micronization of minocycline hydrochloride. *J. Supercrit. Fluid*s, 44, 238–244 (2008)
[37] Li Y, Yu Y, Wang H, et al. Effect of process parameters on the recrystallization and size control of puerarin using the supercritical fluid antisolvent process. *Asian J Pharm Sci,* 11, 281–291 (2016)
[38] He WZ, Suo QL, Hong HL, et al. Supercritical antisolvent micronization of natural carotene by the SEDS process through prefilming atomization. *Ind. Eng. Chem. Res,* 45, 2108–2115 (2006)

Chapter 5

Production of Liposome from Sphingomyelin by Ultrasonic Device under Supercritical Carbon Dioxide

5-1. Introduction

Generally, liposomes are defined as microscopic spherical vesicle in which an aqueous volume is entirely surrounded by a phospholipid membrane and this microscopic spherical vesicle consisted of at least one lipid bilayer. Due to the unique properties of liposomes, it became promising systems for drug delivery. Liposomes may involve a wide variety of hydrophilic and hydrophobic diagnostic or therapeutic agents, providing a larger drug payload per particle and protecting the encapsulated agents from metabolic processes [1–3]. The size of liposomes can range between 25 nm up to several micrometers. Based on the number of lamellae and diameter size, liposomes were classified into several types. They are small unilamellar visicles (SUV), medium–sized unilamellar vesicles (MUV), large unilamellar vesicles (LUV), giant unilamellar vesicles (GUV), oligolamellar vesicles (OLV), large multilamellar vesicles (LMV) and multivesicular vesicles (MVV). The range diameter for SUV and MUV is from 20 to 100 nm and 100 to 500 nm, respectively. The other types of LUV, GUV, OLV, LMV and MVV have a diameter size from few hundred nanometers to several micrometers [2]

Several parameters should be considered during the method selection for liposomes preparation, such as the physicochemical characteristics of the material to be entrapped, choice of liposomal ingredients, nature of the medium in which the lipid vesicles are to be dispersed, effective concentration of the entrapped substance, optimum size and shelf life of the vesicle, and batch–to–batch reproducibility [4,5]. In general, the methods for liposomes preparation were divided into bulk method, where liposomes are generated by transfer of phospholipids from an organic phase into an aqueous phase. The second method is film method, where lipid films are first deposited on a

substrate and subsequently hydrated to result liposomes [6]. Due to the diameter size of liposomes is an important parameter to determine the circulation half–life of liposomes in drug delivery, the size optimization and the lamellarity of liposomes were typically subjected to the method selection for liposomes preparation.

Most of the preparation methods mentioned above use organic solvent. Remaining organic solvent in liposomes may cause problem when they applied to medical field, cosmetics, or beverages. Supercritical carbon dioxide has been used as an alternative solvent in various processes such as decaffeination of green coffee beans and extraction from hops. Here, the preparation of liposomes from sphingomyelin which suspended in an aqueous media was carried out under pressurized carbon dioxide (CO_2) induced by ultrasound. It has been known that CO_2 in supercritical conditions has been widely used as a solvent. CO_2 is a generally recognized as safe (GRAS) solvent and its critical temperature (T_c = 31.06 ^{o}C) and pressure (P_c = 7.38 MPa) are relatively low which helps in preventing thermal degradation during liposomes formation process [7,8]. The advantages of supercritical CO_2 in materials processing include that it is inert, relatively non–toxic, non–flammable, inexpensive, easily available, odorless, tasteless, and environment friendly. CO_2 is also easy to remove from products at atmospheric pressure, accordingly it does not contaminate products. In addition, when the supercritical CO_2 was applied on the liposomes preparation, the small size of liposomes products might be obtained [9–12]. There are several techniques to reduce the size of liposomes products, including sonication, extrusion, and homogenization. Of these, sonication technique, probe sonication or batch sonication, is a simple and a common technique to reduce the size of liposomes [6]. In this process, a very high energy was introduced into the lipid vesicles dispersion, as a result, the MLV are broken down into smaller SUV. In probe sonication process, the tip of a

sonicator is directly introduced into the lipid vesicles dispersion, hence the potential of metal probe contamination may occur due to the metal probe will slough off and contaminate the solution during process [13]. Therefore, in this work, to avoid and to prevent the metal probe contamination, the batch sonication process was used for reducing size of liposomes products.

5-1-1. Sphingomyelin

Sphingomyelin is a type of sphingolipid found in animal cell membranes and can be exploited as an amphiphilic liposome component in the manufacture of liposomes capsule. Here, the fabrication of liposomes from sphingomyelin solution via ultrasonic–supercritical carbon dioxide (CO_2) was studied. The experiments were conducted at temperatures of 40 – 60 ^{o}C and pressures of 10 – 20 MPa in batch process. As a starting material, sphingomyelin powder was dissolved in water distillate. The TEM images indicated that the liposomes products were successfully formed in spherical and spherical–like shape morphologies with bimodal size at 91 – 220 nm and 396 – 955 nm. The liposomes products with smaller diameter were obtained when the experiments were conducted at higher operating pressure. The DLS measurement showed that the size distribution of liposomes products was increased with increasing operating temperature due to the aggregation. Based on the result, this process seems a powerful technique for liposome production technology from sphingomyelin solution for industrial purposes.

5-2. Experimental Section

5-2-1. Materials

Sphingomyelin ($C_{35}H_{75}N_2O_6P$) was obtained from NOF Corporation Japan. It was used without further purification. As one of sphingophospholipids, sphingomyelin is the most abundant sphingolipid and is important structural components of the myelin sheath. It may protect and coat surrounding the nerve fibers. In solution preparation, sphingomyelin was diluted in water distillate that produced by Auto Still WS 200, Yamato, Japan. The sphingomyelin concentration was 0.1 wt%. It should be noted that no sphingomyelin concentration variation was observed during the course of this work. Carbon dioxide (CO_2: 99%) was supplied by Sogo Kariya Sanso, Inc. Japan.

5-2-2. Ultrasonic- Supercritical CO_2 Apparatus

Fig. 5-1 described the liposomes preparation apparatus scheme using ultrasonic – supercritical CO_2. The main apparatus was high pressures pump for CO_2 (PU–2086, Jasco, Japan), an ultrasonic device (Ultrasonic Multi Cleaner W–118, Honda Electronics Company, Japan), acrylic chamber equipped with electric heater, reactor (SUS–316, 80 ml), and back pressure regulator (BPR; AKICO, Tokyo, Japan). The coil preheater made of 1/6 inch

stainless–steel tubing (SUS–316) with 300 cm length was placed in the heating chamber to introduce the CO_2 before entering to reactor. K–type thermocouples were attached in the preheater and placed in the water medium to monitor the temperature during experiment. To monitor the liposomes generation pressures, the analog pressure gauge (GLT–21–25MPa, Migishita Seiki MFG. Co. Ltd., Japan) was assembled on the 1/16 inch stainless–steel tubing (SUS–316) and placed between reactor and BPR.

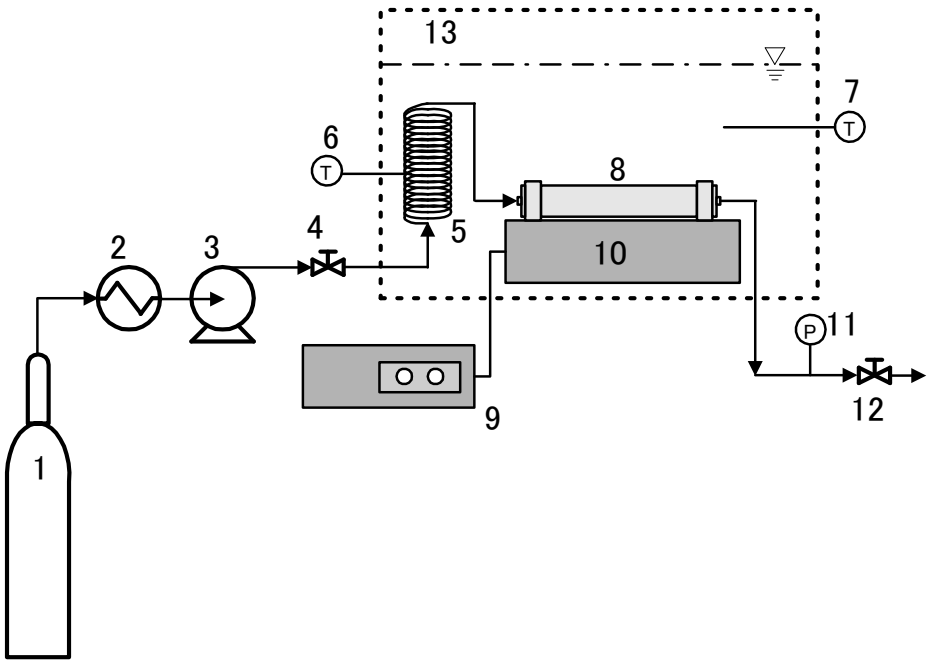

Fig. 5-1: Experimental apparatus scheme: 1. CO_2 cylinder; 2. Chiller; 3. High pressure pump; 4. Needle valve; 5. SUS–316 pre–heater; 6, 7. Temperature monitor; 8. Reactor; 9. Ultrasonic controller; 10. Ultrasonic vibrator; 11. Pressure monitor; 12. BPR; 13.Water bath.

In this work, the liposomes generation from 0.1 wt% sphingomyelin suspension solution by using ultrasonic – supercritical CO_2 was carried out at temperatures of 40 – 50 °C and pressures of 10 – 20 MPa in batch process. The liposomes generation process can be explained briefly as follow. Initially, the power of heating chamber was switched on to heat the water medium including preheater to a desired temperature. Once the desired temperature was achieved, the stainless–steel reactor loaded by 60 ml sphingomyelin solution was immersed into the acrylic chamber. This reactor was equipped with removable threaded covers on both sides; these included stainless steel filters (0.1 – 1.0 μm). In order to remove the air, the reactor was purged by CO_2 gas and immediately sealed. Next, CO_2 was pumped into the liposomes preparation apparatus system via the 1/16 inch stainless–steel capillary tube at a desired pressure. A BPR was employed to keep a constant pressure during liposomes generation process. The time required to heat the reactor from room temperature to the desired temperature (the reactor temperature) was 5 – 8 min. Thereafter, ultrasonic was applied (28 kHz) in the liposomes preparation apparatus for 60 min at each experimental condition. After the process was completed, the CO_2 was slowly depressurized to atmospheric pressure. Then the solution products were collected in the bottles and stored in a refrigerator until further analysis.

To characterize the liposomes products, transmission electron microscopy (TEM) was carried out using negative staining method on a Hitachi H9000NAR microscope equipped with a cold field–emission gun. The acceleration voltage was 300 kV, and the TEM images were captured by CCD

(charge–coupled device) camera. Prior to characterization, the liposomes products were diluted 10 times with water and then drop cast onto an elastic carbon–coated copper grid. It was stored in a desiccator overnight at room temperature to desorb atmospheric contaminants. The particle size distribution of the liposomes products was determined by dynamic light scattering analysis (DLS; Malvern Instruments, Malvern, England).

5-3. Results and Discussion

Fig. 5-2 shows the TEM images of the structural morphology of liposomes products generated under supercritical CO_2 at temperature of 40 ^{o}C with various pressures. It was well known that liposome preparation is simply understood and it can be produced from a various lipids and lipid mixtures, with phospholipids the most commonly used. The different preparations of liposomes were usually described by TEM. As shown in this figure, many spherical and spherical–like particles morphologies of liposomes products were found at each experimental condition. At low CO_2 pressure (10 MPa), the spherical particles of liposomes products were obtained dominantly. Conversely, the liposomes products with spherical–like particles morphology were found prominently at higher CO_2 pressure (20 MPa). It seems that the liposomes products with spherical shape morphologies were transformed into non–spherical shape morphologies with increasing CO_2 pressures. At these conditions, the CO_2 pressure as a driving force may press to change the

liposome volume thereby changing the shape of liposomes products [14–16]. Choi *et al.* [15] informed that the osmotic pressure most likely led to the liposome morphological changes such as shrinkage, fission, swelling, and fusion of membranes. Hayashi *et al.* [16] reported that the liposome underwent deformation from a spherical shape to an ellipsoid shape and then to a lemon–like shape morphology when the pressure was applied on the liposomes solution. They informed that no changes were found in the morphology of liposomes before the application of pressure. On the contrary, the boundary between the central spherical part and the protruding parts led to obscure to result indefinite shapes of liposomes became with flabby membranes when the pressure was applied at 0.1 to 60 MPa. Judging from the results, it could be said that the morphologies of liposomes products seemed influence with changing operating pressure.

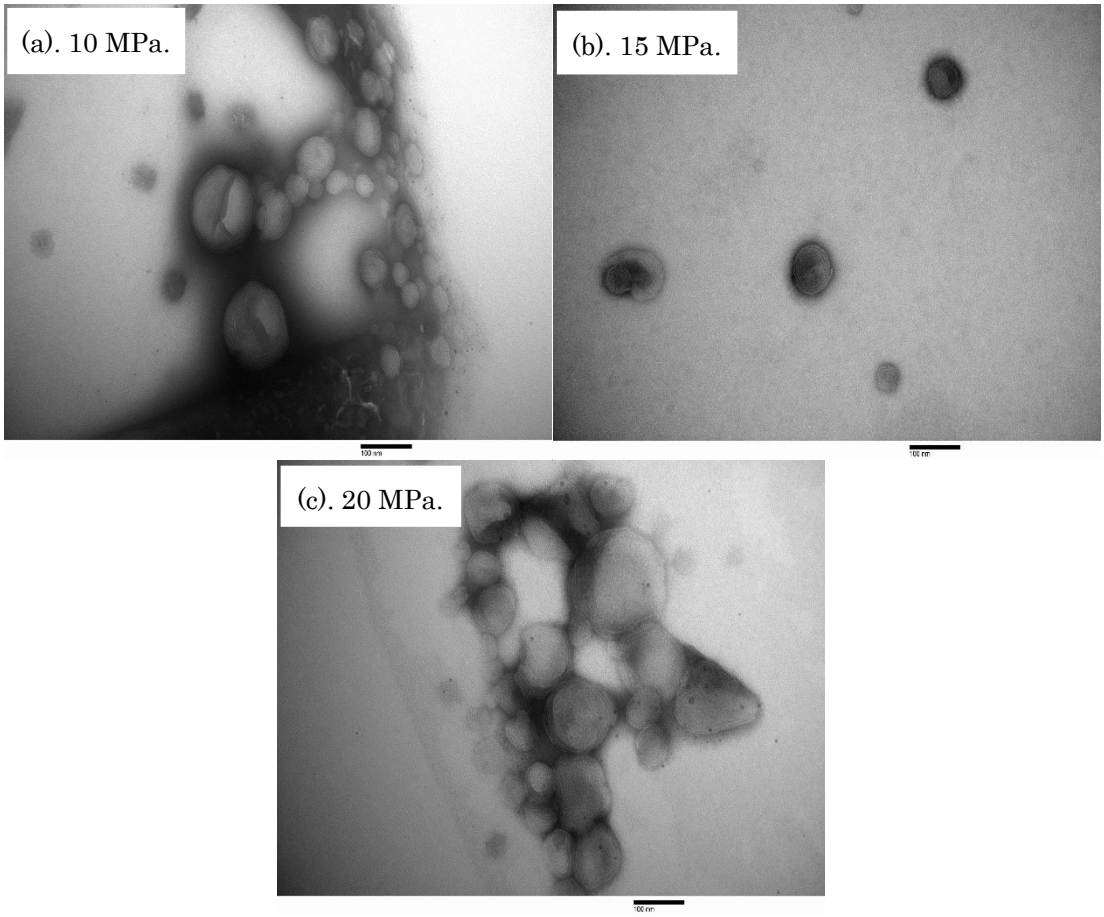

Fig. 5-2: TEM images of liposomes products obtained at temperature of 40 °C with various CO_2 pressures.

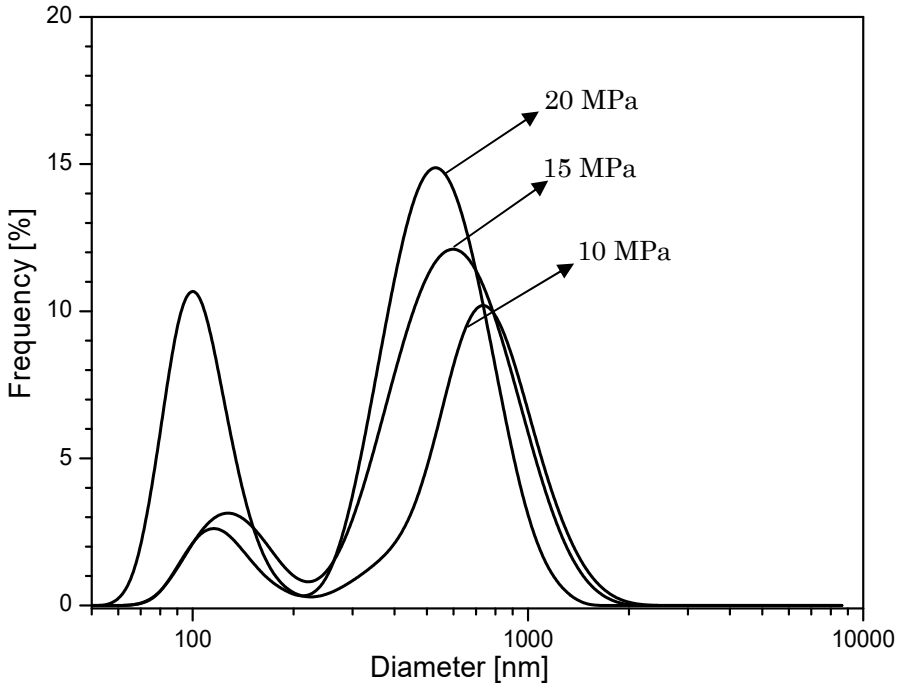

Fig. 5-3: The liposomes products size distribution obtained at temperature of 40 °C with various CO_2 pressures.

Visually (see **Fig. 5-2**), operating pressure did not seem to have a perceivable effect on the size of liposomes products. They seem to have a similar size at each operating condition. In order to understand the diameter size distribution of liposomes products, the sphingomyelin solution after treatment by ultrasonic – supercritical CO_2 was loaded in the cuvette and placed in the holder of DLS equipment. This analysis is common technique to quantify the small–molecule aggregates size by measuring the time–

dependent fluctuation of scattering intensity of a coherent light source illuminating particles suspended in solution. **Fig. 5-3** showed the diameter size distribution of liposomes products generated at temperature of 40 ^{o}C and CO_2 pressures of 10, 15, and 20 MPa. The double–peaked (bimodal) diameter size distribution of liposomes products were found at each operating condition. Both peaks seem to approach at a smaller size around 91 – 122 nm and a larger size around 396 – 712 nm. It seems that the liposomes products in diameter ranges of 91 – 122 nm and 531 – 1106 nm were formed dominantly at 10 MPa CO_2 pressure. At 20 MPa CO_2 pressure, the diameter ranges of liposomes products were 105 – 122 nm and 396 – 712 nm. Thus, it could be said that although the CO_2 pressure did not give strong effect on the liposomes products size distribution, the narrower liposomes products size distributions were obtained with increasing CO_2 pressure at the same operating temperature. From this figure, it could be seen that the liposomes products also had smaller diameter when the experiments were conducted at higher operating pressure. In this work, the liposomes preparation under supercritical CO_2 without applied ultrasonic or by sonication process at room temperature did not perform. Hence, there was no comparison result between liposomes products formed by supercritical CO_2 without applied ultrasonic treatment or by the conventional sonication process and ultrasonic – supercritical CO_2 process. However, Karn *et al.* [12] informed that liposomes products prepared with supercritical CO_2 gave relatively much smaller and more homogenous in size. They observed that low CO_2 pressure (8 MPa) and low operating temperature (<35 ^{o}C) were insufficient conditions for producing

liposomes. Similar results were also reported by Otake *et al.* [9] and Kadimi *et al.* [10] when they conducted experiments for preparation of liposomes using an improved supercritical reverse phase evaporation method and in vitro studies on liposomal amphotericin B obtained by supercritical CO_2–mediated process, respectively.

As informed above that the experimental temperature for liposomes preparation under ultrasonic – supercritical CO_2 were 40 to 60 ^oC. To reach the desired operating temperature, the reactor which has been filled by sphingomyelin solution was submerged in the acrylic chamber containing water medium. Due to the application of the ultrasound path–length may give an effect on the temperature rise of water medium during experiments, the water from temperature–controlled bath was circulated by using water pump to maintain the desired temperature. **Fig. 5-4** showed the TEM images of liposomes products when the experiments were carried out at a constant pressure (20 MPa) with various operating temperatures from 40 to 60 ^oC. It has been known that the change of environmental temperature led to stimulate and cause shape transformations of liposomes [17–19]. This change may change the spontaneous curvature globally on the whole surface of the lipid vesicle. Jelger and Siewert [20] explained that the liposomes radius may increase with increasing the environment temperatures and hence the curvature difference between the two monolayers decreases. They also informed that at higher environment temperatures the effective volume of the tails increases due to the increased thermic motions, resulting the lipid

vesicles effectively more inverted cone shaped. In other words, with increasing environment temperatures, the decreased volume of liposomes reduces and the spherical liposomes changes its shape. Zook and Vreeland [21] also informed that environment temperature may change the lipid vesicle size primarily as a result of its effect on the ratio of the membrane bending elasticity modulus to the line tension. However, as shown in **Fig. 5-4**, the morphologies of liposomes products did not change obviously with increasing operating temperature. It seems that the morphologies of them were spherical and spherical–like shapes at each experiment. This phenomenon might be due to the physical properties of water media was not much change with increasing environment temperature. As a result, the similar morphologies of liposomes products were found at each experimental condition. At these environment temperatures, Zook and Vreeland [21] reported that the viscosity, free energy, and diffusion coefficients of water media which modulated by the changing environment temperatures may not have enough ability to give a sufficient effect for changing the liposomes products morphologies. Liu and Iglic [18] also informed that although the deformation of liposome morphology might occur by the changing environment temperatures, the shape of liposome morphology depended on the properties and the concentration of the components.

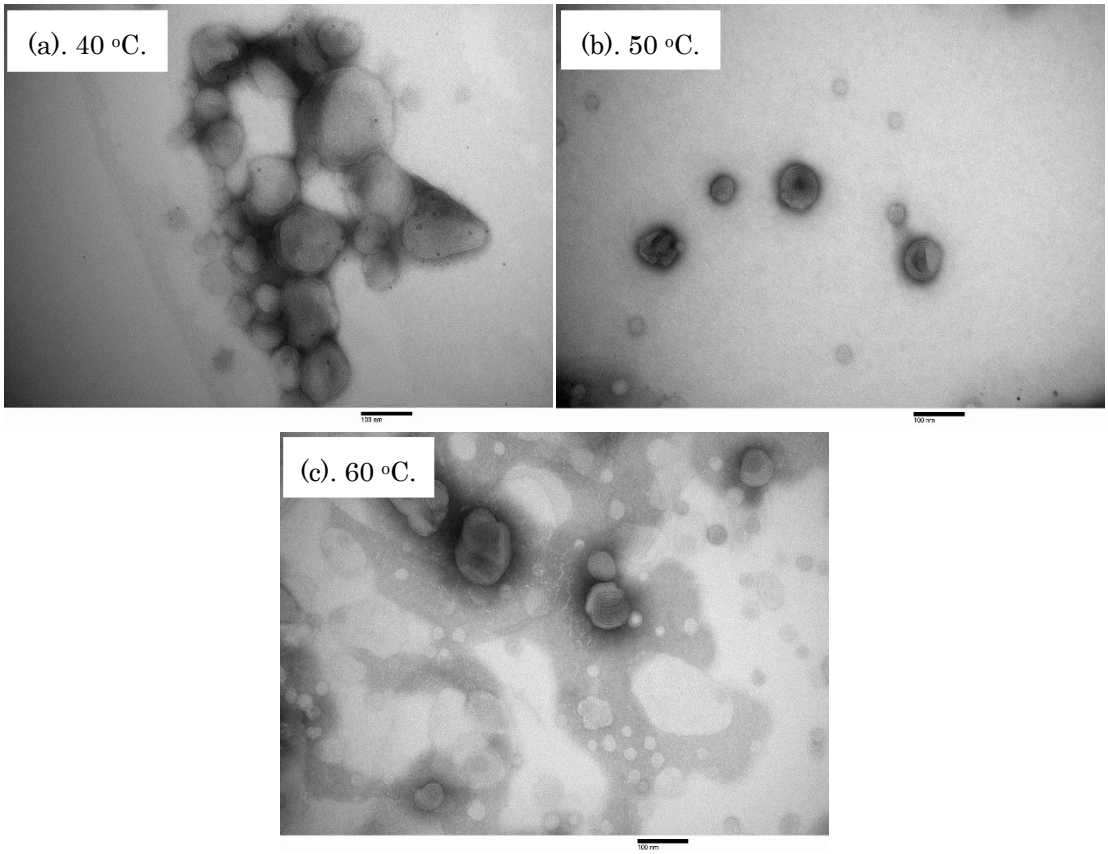

Fig. 5-4: TEM images of liposomes products obtained at CO_2 pressure of 20 MPa with various operating temperatures.

Similar to the phenomenon in shape of liposome morphology, the changing environment temperatures will also affect to the size distribution of liposomes products [21]. Zook and Vreeland [21] explained that there were three ways for affecting temperature on the size of liposomes during process: first, by changing the free energy and the diffusion coefficients; second, by changing the medium viscosity; and third, by changing the membrane elasticity at or below the transition temperature and by changing the line tension. **Fig. 5-5** showed the size distribution of liposomes products obtained

at 20 MPa CO_2 pressure with operating temperatures of 40 – 60 °C. It was well known that beside the decreasing medium density and viscosity contribute in the reduction process of liposome sizes, the higher operating temperature will also lead to in effective lipid vesicles dispersion and result the smaller size of liposomes [22]. However, as shown in **Fig. 5-5**, the size distributions of liposomes products seem increased slightly with increasing operating temperature. At 40 °C, the liposomes products had diameter ranges of 105 – 122 nm and 396 – 712 nm. Their diameter ranges increased to 164 – 220 nm and 615 – 955 nm when the operating temperature was increased to 60 °C at the same CO_2 pressure. It could be explained that the aggregation of liposomes products might be occur. The operating temperature was known as one of the factors that can affect the degree of aggregation liposomes during formation process [23,24]. Liposomes will be produced only at environment temperatures higher than the main transition temperature of the phospholipid which used as a starting material and has a significant effect on the size of liposomes products. The phase transition temperature ranges of all naturally occurring sphingomyelins is around 30 – 45 °C [25]. Unfortunately, the heat energy of the lipid vesicle membrane at high temperatures is sufficient to overcome the potential barrier of aggregation, consequently the liposomes products in the solution system tends towards aggregation. The aggregation process commonly was initiated at an environment temperature near to that for phase transition into hexagonal phase [23]. As a result, the size distribution of liposomes products obtained by DLS measurement is increased with increasing operating temperature range studied.

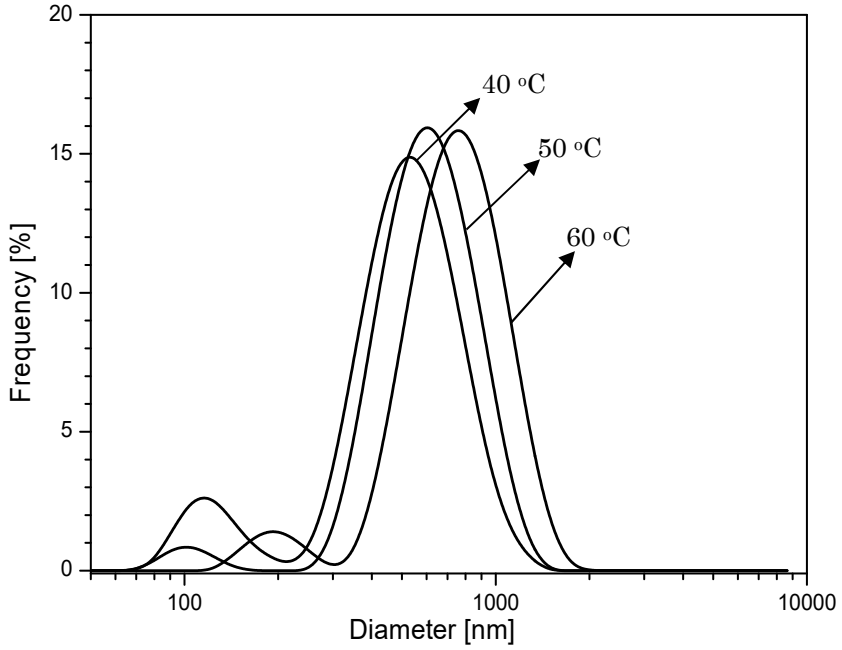

Fig. 5-5: The liposomes products size distribution obtained at CO_2 pressure of 20 MPa with various operating temperatures.

5-4. Conclusions

The production of lipid vesicles from sphingomyelin solution via ultrasonic–supercritical CO_2 has been demonstrated. The experiments were carried out at temperatures of 40 – 60 °C and pressures of 10 – 20 MPa in batch process. The sphingomyelin powder dissolved in distillate water at 0.1 wt% was used as a starting material. At each experiment, the applied ultrasonic power was 28 kHz for 60 min. The TEM images showed that the

liposomes products were successfully produced in spherical and spherical–like shape morphologies with size less than 1 μm. The liposomes products with smaller diameter were obtained when the experiments were conducted at higher operating pressure. The DLS analysis showed that the size distribution of liposomes products increased with increasing operating temperature due to the aggregation. Finally, it could be said that this process seems a powerful technique and to be an apt for liposome production from sphingomyelin solution.

Refferences

[1] Daraee, H., Etemadi, A., Kouhi, M., Alimirzalu, S., Akbarzadeh, A., Application of liposomes in medicine and drug delivery, Artif. *Cells Nanomed. Biotechnol.*, 44, 1, 381–391 (2016)

[2] Pattni, BS., Chupin, VV., Torchilin, VP., New developments in liposomal drug delivery, *Chem. Rev.*, 115, 19, 10938–10966 (2015)

[3] Alavi, M., Karimi, N., Safaei, M., Application of Various Types of Liposomes in Drug Delivery Systems, Adv. Pharm. Bull., 7, 1, 3–9 (2017)

[4] Gomez–Hens, A., Fernandez–Romero, JM., Analytical methods for the control of liposomal delivery systems, *Trends Anal. Chem.*, 25, 2, 167–178 (2006)

[5] Mozafari, MR., Johnson, C., Hatziantoniou, S., Demetzos, C., Nanoliposomes and their applications in food nanotechnology, *J. Liposome Res.*, 18, 4, 309–327 (2008)

[6] Patil, YP., Jadhav, S., Novel methods for liposome preparation, *Chem. Phys. Lipids*, 177, 8–18 (2014)

[7] Herrero, M., Mendiola, JA., Cifuentes, A., Ibanez, E., Supercritical fluid extraction: Recent advances and applications, *J. Chromatogr. A*, 1217, 16, 2495–2511 (2010)
[8] Goto, M., Kanda, H., Wahyudiono, Machmudah, S., Extraction of carotenoids and lipids from algae by supercritical CO_2 and subcritical dimethyl ether, *J. Supercrit. Fluids*, 96, 245–251 (2015)
[9] Otake, K., Shimomura, T., Goto, T., Imura, T., Furuya, T., Yoda, S., Takebayashi, Y., Sakai, H., Abe, M., Preparation of liposomes using an improved supercritical reverse phase evaporation method, *Langmuir*, 22, 6, 2543–2550 (2006)
[10] Kadimi, US., Balasubramanian, DR., Ganni, UR., Balaraman, M., Govindarajulu, V., In vitro studies on liposomal amphotericin B obtained by supercritical carbon dioxide–mediated process, *Nanomed.*, 3, 4, 273–280 (2007)
[11] Meure, LA., Foster, NR., Dehghani, F., Conventional and dense gas techniques for the production of liposomes: a review, *AAPS Pharm. Sci. Tech.*, 9, 798–809 (2008)
[12] Karn, PR., Cho, W., Park, HJ., Park, JS., Hwang, SJ., Characterization and stability studies of a novel liposomal cyclosporin A prepared using the supercritical fluid method: comparison with the modified conventional Bangham method, *Int. J. Nanomed.*, 8, 365–377 (2013)
[13] Bhuvana, M., Dharuman, V., Tethering of spherical DOTAP liposome gold nanoparticles on cysteamine monolayer for sensitive label free electrochemical detection of DNA and transfection, *Analyst.*, 139, 10, 2467–2475 (2014)
[14] Nomura, F., Honda, M., Takeda, S., Inaba, T., Takiguchi, K., Itoh, TJ., Ishijima, A., Umeda, T., Hotani, H., Morphological and topological transformation of membrane vesicles, *J. Biol. Phys.*, 28, 2, 225–235 (2002)
[15] Choi, HJ., Song, JM., Bondy, BJ., Compans, RW., Kang, SM., Prausnitz, MR., Effect of osmotic pressure on the stability of whole inactivated influenza vaccine for coating on microneedles, *PLoS one*, 10, 7, e0134431 (2015)
[16] Hayashi, M., Nishiyama, M., Kazayama, Y., Toyota, T., Harada, Y., Takiguchi, K., Reversible morphological control of tubulin–encapsulating giant liposomes by hydrostatic pressure, *Langmuir*, 32, 15, 3794–3802 (2016)
[17] Yaghmur, A., De Campo, L., Sagalowicz, L., Leser, ME., Glatter, O., Emulsified microemulsions and oil–containing liquid crystalline phases, *Langmuir*, 21, 2, 569–577 (2005)
[18] Liu, AL., Iglic, A., Advances in Planar Lipid Bilayers and Liposomes, Volume 10, 1st Edition, *Academic Press*, (2009)
[19] Monteiro, N., Martins, A., Reis, RL., Neves, NM., Liposomes in tissue engineering and regenerative medicine, *J. R. Soc. Interface*, 11, 101, 20140459 (2014)

[20] Risselada, HJ., Marrink, SJ., Curvature effects on lipid packing and dynamics in liposomes revealed by coarse grained molecular dynamics simulations, *Phys. Chem. Chem. Phys.*, 11, 12, 2056–2067 (2009)
[21] Zook, JM., Vreeland, WN., Effects of temperature, acyl chain length, and flow–rate ratio on liposome formation and size in a microfluidic hydrodynamic focusing device, *Soft Matter,* 6, 6, 1352–1360 (2010)
[22] Justo, OR., Moraes, AM., Analysis of process parameters on the characteristics of liposomes prepared by ethanol injection with a view to process scale–up: effect of temperature and batch volume, *Chem. Eng. Res. Des.*, 89, 6, 785–792 (2011)
[23] Torchilin, VP., Omelyanenko, VG., Lukyanov, AN., Temperature dependent aggregation of pH–sensitive phosphatidyl ethanolamine–oleic acid–cholesterol liposomes as measured by fluorescent spectroscopy, *Anal. Biochem.*, 207, 1, 109–113 (1992)
[24] Toh, MR., Chiu, GN., Liposomes as sterile preparations and limitations of sterilisation techniques in liposomal manufacturing, *Asian J. Pharm. Sci.*, 8, 2, 88–95 (2013)
[25] Li, J., Wang, X., Zhang, T., Wang, C., Huang, Z., Luo, X., Deng, Y., A review on phospholipids and their main applications in drug delivery systems, *Asian J. Pharm. Sci.*, 10, 2, 81–98 (2015)

Chapter 6

Summary and Conclusions

6-1. Summary

There are various usages of supercritical fluid technology.
The most extensively used field is the extraction and purification of nutraceutical and ingredients from natural products. The extracted products have been used in the field of foods, beverages, and supplemental foods. Since supercritical carbon dioxide is a tasteless, odorless, and safe solvent, it is suitable for extraction and separation for these. The other field is fine particle formation of natural materials. There are many technologies for particle formation using supercritical fluid. In this study, we used supercritical anti-solvent precipitation where supercritical CO_2 is used as an anti-solvent. We also studied to make liposome in supplemental CO_2 by using ultrasonic power.

6-1-1. Extraction of functional component

In Chapter 2, extraction method was evaluated for plant biomatrix, grains of paradise, using supercritical carbon dioxide. The grains of paradise are mainly used as spices. We studied extraction and separation of ingredients contained in seeds of plants under various conditions.

In that case, it was shown that the important parameter is the density of supercritical carbon dioxide. Changing the extraction temperature or pressure is effective in selectively separating the components.

Results of FT-IR analysis showed that phytochemicals in the seed was extracted by supercritical carbon dioxide. They were gingerols, shogaols and paradols. They have action to prevent the growth of pancreatic tumor in human body. Therefore, for grains of paradise, it pharmacological competent ingredients can be extracted with supercritical carbon dioxide.

6-1-2. Production of lycopene nanoparticles

Lycopene has a strong antioxidant special made, and attracts attention due to its anti-arteriosclerotic effect and anti-cancer action.
In this study, we aimed to separate them without breaking their characteristics.

The effect of the *Z*-isomer content on particle production of lycopene by the solution-enhanced dispersion by supercritical fluids process was evaluated. Using the thermal isomerization and filtering technique, lycopene containing a large amount of *Z*-isomers was prepared from (all-*E*)-lycopene. On the other hand, when using lycopene containing a large amount of the *Z*-isomers, the lycopene particles became significantly finer compared with those obtained using (all-*E*)-lycopene. Interestingly, despite the *Z*-isomer content of the raw materials, the obtained lycopene particles were primarily in the thermodynamically stable all-*E* isomer. Therefore, the *Z*-isomerization pre-treatment of lycopene is very effective to obtain uniform, stable, and fine particles using SEDS precipitation.

6-1-3. Micro-particulation of acetaminophen

Acetaminophen is a drug widely used in the world. The fabrication of acetaminophen particles via supercritical antisolvent process with CO_2 as an antisolvent was studied. The experiments were conducted at temperatures and presser. As a starting material, acetaminophen powder was dissolved in dimethylformamide (DMF). Results of UV–vis spectrophotometry and GC–MS (gas chromatography mass spectrometry) analysis showed that there was no remaining DMF solvent in the acetaminophen particles products. It indicated that CO_2 has successfully removed DMF from acetaminophen particles products. The surface characterization by using fourier transform infrared spectroscopy (FT–IR) showed that the CO_2 solvent did not impregnate to the acetaminophen particles products. Results from scanning electron microscope (SEM) images showed that the acetaminophen particles products were successfully prepared in non–spherical shape morphologies with size less than 1 μm. Based on the result, this process seems a powerful method to modify the acetaminophen powder physically such as particle size reduction.

6-1-4. Production of liposome capsule using supercritical carbon dioxide

Sphingomyelin is a sphingolipid found in animal cell membranes. Here, the fabrication of liposomes from sphingomyelin solution via ultrasonic–

supercritical carbon dioxide was studied. As a starting material, sphingomyelin powder was dissolved in water distillate. The TEM images indicated that the liposomes products were successfully formed in spherical and spherical–like shape morphologies with bimodal size. The liposomes products with smaller diameter were obtained when the experiments were conducted at higher operating pressure. The DLS measurement showed that size distribution of liposomes products was increased with increasing operating temperature due to the aggregation. Based on the result, this process seems a powerful technique for liposome production technology from sphingomyelin solution for industrial purposes.

This technique is a powerful technique for producing safe liposome capsules and will be used in various fields in the future.

6-2. Conclusions

In this study, various technologies for extraction and fine particle formation were developed using supercritical carbon dioxide. These technologies can be used in wider fields. Some techniques are being carried out commercially in the world. It is an advantage that supercritical carbon dioxide can be used as green solvent instead of organic solvent. Furthermore, after extraction and separation, carbon dioxide returns to gas at normal temperature and pressure, so it can be recovered and there is no residue in the products. Therefore, supercritical fluid technology will be a promising

green technology for sustainable development.

Acknowledgement

I would like to express my sincere gratitude to my supervisors, Professor Motonobu Goto (Department of Materials Process Engineering) and Assistant Professor Hideki Kanda (Department of Materials Process Engineering). I especially would like to express my deepest appreciation to Dr. Wahyudiono (Department of Materials Process Engineering) and Dr. Siti Machmudah (Institut Teknologi Sepuluh Nopember, Indonesia) and Dr. Masaki Honda (Graduate School of Bioagricultural Sciences) for their considerable encouragement to make my study unforgettable. I gratefully acknowledge the research of past and present members of our laboratory.

I am grateful to Dr. Ryuich Fukuzato (SCF Techno-Link, Inc., former Guest Professor of Nagoya University and Kumamoto University), because he gave me a lot of advices and guidance. Special thanks to Mr. Tatsuhiko Kon (Toyo Hakko Co., Ltd.) for their valuable cooperation in my experiments.

I wish to thank Professor Koyo Norinaga (Department of Chemical Systems Engineering), Professor Seiichi Takami (Department of Materials Process Engineering), and Professor Jyun Onoe (Department of Energy Engineering) as a thesis examiner.

Chiho Uemori

List of Publications

1. Maiko Ono, Yukihiro Kawamoto, Chiho Uemori, Wahyudiono, Hideki Kanda, Motonobu Goto, Extraction of Phytochemicals from Grains of Paradise Using Supercritical Carbon Dioxide, Engineering Journal, 21, 4, 53-64 (2017)

2. Tomohiko Kodama, Masaki Honda, Ryota Takemura, Chiho Uemori, Wahyudiono, Hideki Kanda, Motonobu Goto, Effect of Z-isomer Content on Nanoparticle Production of Lycopene Using Solution-Enhanced Dispersion by Supercritical Fluids (SEDS), The Journal of Supercritical Fluids, 133, 291-296 (2018)

3. Chiho Uemori, Tsubasa Katsube, Siti Machmudah, Wahyudiono, Hideki Kanda, Keiji Yasuda, Motonobu Goto, Production of Liposome from Sphingomyelin by Ultrasonic Device under Supercritical Carbon Dioxide, Asian Journal of Applied Sciences, 5, 5, 1042-1048 (2017)

4. Chiho Uemori, Tomohiko Kodama, Siti Machmudah, Wahyudiono, Hideki Kanda, Motonobu Goto, Crystallization of Acetaminophen in Nano/Micro Scale Using Swirl Mixing Micro Device Under Pressurized Carbon Dioxide, ARPN Journal of Engineering and Applied Sciences, (accepted for publication)